University of Stavanger

Faculty of Science and Technology

MASTER'S THESIS

Study program/ Specialization: **Offshore Technology/ Marine and Subsea Technology**	Spring semester, 2019 **Open** / Restricted access
Writer: **Timur Timerbaev**	…………………………………………… (Writer's signature)

Faculty supervisor: **Professor Ove Tobias Gudmestad**

External supervisor: **Professor Anatoly Borisovich Zolotukhin**

Thesis title:

«Subsea Pipeline Design Features on the Russian Shelf Conditions»

Credits (ECTS): 30

Key words: Arctic, subsea pipelines, pipeline installation, pipeline trenching, Shtokman trunk pipeline,pipeline wall thickness calculation, on-bottom stability analysis, stress-strain state of pipeline.	Pages: 89 Stavanger, June 15, 2019

Title page for Master's Thesis
Faculty of Science and Technology

Abstract

Today in Russia, more than 75% of the explored onshore oil and gas fields are involved in the development, and their reserves have been produced at least by half. New discovered deposits are less and less, and their resources are several times less than 20-30 years ago. Discovered, but not developed, offshore fields, by contrast, are classified as large or even giant [32]. Therefore, Russian oil and gas companies are facing the task of sharply intensifying their activities on the shelf in the near future.

During the development of offshore fields, one of the main issues is the choice of transportation method of the extracted products. Today, hydrocarbons are transported either by tanker or by pipeline. For several reasons, preference is given to pipelines: the offshore pipeline, unlike a tanker, allows uninterrupted supply of hydrocarbons to the shore, regardless of weather conditions, and in addition, ship accidents are more dangerous than on pipelines.

All Russian oil and gas shelves are located in freezing seas of Arctic. The region of the Arctic seas, is characterized by its harsh climatic and hydrometereological conditions, which require a special approach in the design of subsea pipelines.

This thesis discusses the main features in the construction of underwater pipelines in the conditions of the Russian Arctic region. Also in Master thesis such stages of designing subsea pipelines as the choice of the minimum wall thickness of the pipeline, the determination of the required thickness of the weighting concrete coating are shown. In addition, the analysis of the stress-strain state of the pipeline during its installation is conducted. The calculations were carried out evidence from the trunk pipeline for the Shtokman gas condensate field (SCGF – Teriberka).

Acknowledgements

I am very grateful to Ove Tobias Gudmestad, a professor from University of Stavanger, for his professional leadership, motivation, helpful advices and constant support. Without his great experience and deep knowledge in the marine operations, my work would not be completed. I would like to thank him for his active participation in the writing of master thesis and for his hospitality.

Special thanks to Professor Anatoly Zolotukhin and Associate Professor Vladimir Balitsky from the Gubkin University. Throughout the entire education period, they provided all the students of the Russian-Norwegian master program with all the necessary information, as well as provided assistance in writing of master's thesis.

Finally, I want to thank my family, who supported me in writing my thesis throughout the entire study period.

Content

List of Figures

List of Tables

List of Abbreviations

LNG   Liquefied Natural Gas

FSBI   Federal State Budgetary Institution

JSC   Joint-stock Company

PDP   Pilot Development Planning

FOIROT   Fixed Offshore Ice-resistant Off-loading Terminal

ROV   Remotely Operated Vehicle

HDD   Horizontal Directional Drilling

TSHD   Trailer Suction Hopper Dredge

BHD   Backhoe Dredge

CSD   Cutter Suction Dredger

SGCF   Shtokman Gas Condensate Field

DNV   Det Norske Veritas

UGSS   Unified Gas Supply System

UO   Pipe fabrication process for welded pipes

TRB   Three Roll Bending

ERW   Electric Resistance Welding

UOE   Pipe fabrication process for welded pipes, expanded

SDAG   Shtokman Development AG

DSS   Duplex Stainless Steel

SLS   Serviceability Limit State

ULS   Ultimate Limit State

FLS   Fatigue Limit State

ALS   Accidental Limit State

DEG   Diethylene glycol

MEG   Monoethylene glycol

Introduction

Nowadays Russia meets a need of commercial development of oil and gas resources at the continental shelf. Russia possesses 22% of the World's Water zone, 80-90 % thereof is considered to be prospective for the extraction of hydrocarbon resources. About 85 % of those resources is placed in the Arctic shelf, especially in the Kara and the Barents seas [31].

During the development of offshore fields, one of the main issues is the choice of transportation method of the extracted products. Today, hydrocarbons are transported either by tanker or by pipeline.

The advantages of oil and gas transportation by subsea pipelines, comparing to the tankers, lie in climate influence absence as well as in the ability to remote control and a low probability of environmental contamination. Also, these advantages include an ability of constant product transportation and pipeline oil and gas storage.

In general, the construction of subsea pipelines in the Arctic area demands solution of a number of tasks, including technical, technological and organizational ones. Those are connected with challenges caused by natural conditions as well as the remoteness from the industrial areas, by the absence of well-developed infrastructure and rigid environmental requirements.

The main objectives of this master's thesis include:

- Analysis of the prospects for the development of the Russian Arctic shelf;
- Analysis of the potential conditions for the construction of offshore pipelines in the Arctic;
- Review of existing project of subsea pipeline construction in the Arctic;
- Investigation of subsea pipeline installation and operation features in the Arctic shelf;
- Calculation of pipeline design parameters for the Shtokman gas condensate field.

1. Analysis of Development for Arctic Russian Shelf

Last years the Arctic Ocean has been an object to the monitoring of many countries. The ground for that is a discovery of hydrocarbon resources in the Arctic waters. These resources are superior to such ones in the Persian Gulf [8].

The square of the Arctic Ocean equals to 14.8 million km^2. This territory is divided into 5 sectors, which belong to Russia, the USA, Canada, Norway and Denmark. Russia has about 4 million km^2, which makes more than a half of the Arctic Ocean seaboard. This region comprises the eastern part of the Barents Sea, the Kara Sea, the Laptev Sea, the East Siberian Sea, the western part of the Chukchi Sea and its islands [8]. The distribution of the hydrocarbon resources in this area is illustrated in the Figure 1.1.
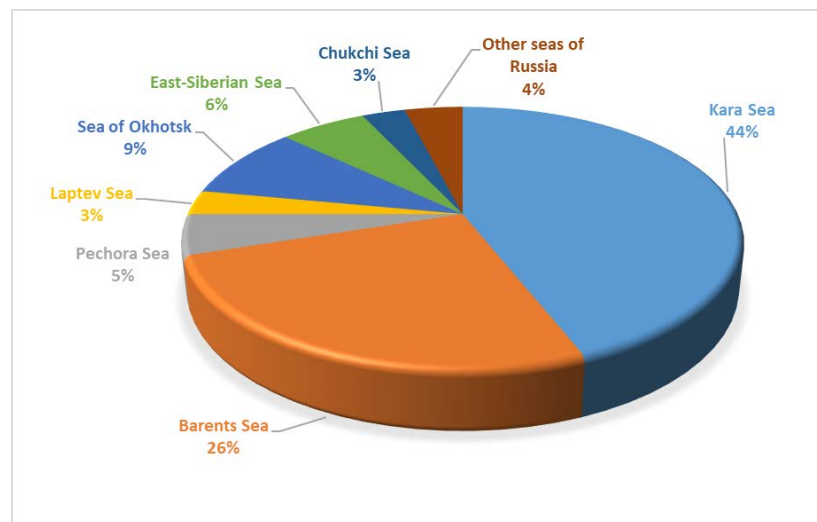
Figure 1.1. Distribution of Initial Total Resources in the Sea Areas of Russia [13]

The first estimation of oil and gas reserves in the Russian Arctic shelf was conducted in 1969. As a result, the territory showed high prospectivity to be a source of oil and gas. 1979 onwards exploration works took place in the Arctic shelf with gathering frequency and activity. All this was a result of oilfield development on the Kolguyev Island in the Pechora Sea. In 1993 the first international Russian Arctic shelf exploration conference took place, at which the importance and practical character of the shelf exploration was underlined. Nowadays one can evidence works over the development projects of Pechora, Barents and Kara sea shelf [13].

The structure of the total initial resources of the hydrocarbons extracted in the Arctic shelf zone of Russia comprises 13016 million tons (MT), free gas - 95118 billion m^3(Bm^3), the condensate - 4504 MT. Generally, it is accumulated in the East of the Arctic. Dissolved and free gas make over

85 % of total initial hydrocarbon resources [20]. The distribution of it in the Arctic zone is given in the Table 1.1.

Table 1.1. Total initial hydrocarbon resources in the Arctic zone of Russia [20]

Arctic sector of Russia	Oil		Dissolved gas		Free gas		Condensate		Total amount of hydrocarbons	
	MT	%	BT	%	Bm^3	%	MT	%	MT	%
Onshore	20030	60.6	2606.8	67.4	113515	54.4	7838.5	63.5	143989	55/8
Offshore	13016	39.4	1262.7	32.6	95118.5	45.6	4504.2	36.5	113902	44.2
Total	33046	100	3796.7	100	208633	100	12342.7	100	257892	100

As of 1 January 2015 in the Arctic sea shelf 20 subsea and 13 transit oil and gas fields were explored. Nowadays «Gazprom», «Rosneft» and «Novatek» conduct geological exploration in this area under the licenses obtained.

An important project on the gas resource development in the Arctic is «Yamal LNG». Its resource base is Yuzhno-Tambeyskoye field situated in the Northeast from Yamal Peninsula, namely nearby Ob Bay. The proved and probable reserves include about 27 Bm^3 of gas a year available for extraction for over 20 years [20].

1.1. Barents-Kara Region

The Barents and Kara are the largest seas (the Barents is 884.8 thousand square kilometers, the Kara - 880 thousand square kilometers) situated in the border shelf of the Arctic Ocean. Their common features are adverse climatic and natural conditions, the vicinity with the Atlantic Ocean, a relatively free access to its warm waters and the influence of the Arctic Ocean [20].

According to the FSBI «All-Russian Research Geological Oil Institute», recently explored fields in the eastern Arctic shelf borders (Kara and Barents area) comprise 9965 m^3 of A+B+C+C2 gas resources. According to different estimations, gas potential of the Arctic region field is 92-100 trillion m^3. It is essential that these reserves are not uniformly distributed in the shelf. The greatest bulk of reserves is situated in the northeastern seas. According to the estimations of experts, gas reserves of the Barents Sea are far less than those of the Kara Sea. Gas reserves of the Barents Sea are timed of the Jur and Trias sediments. The Kara gas reserves are dated to the Lower Cretaceous

and to the Cenomanian periods, the peripheral reserves were formed in the higher level of the Middle Jurassic period [27].

Based on the explored fields, it is possible today to arrange two gas and one oil producing regions. The first gas-producing region can be in the central part of the Barents Sea and it can combine Shtokmanovskoye, Ludlovskoye and Ledovoye fields. These reserves provide gas extraction no less than 100 Bm^3 a year. The second gas producing region is situated in the Kara Sea, namely near the Yamal Peninsula. It combines Rusanovskoye and Leningradskoye fields [20].

In the early of the 21st century the search for new gas fields was connected with the geological exploration on Ob and Tar bays in the Kara Sea, where large Kamenomysskoe-More, Severo-Kamenomysskoe, Yurkharovskoye fields are situated. In addition, there were explored offshore parts of Semakovskoe, Antipayutinskoye, Tota-Yakhinskoe fields, which were previously explored onshore. This provided the growth of gas reserves in the bays to 2 trillion m^3 [20].

«Gazprom» conducts designing of the Kamenomysskoe-More field in Ob bay, which has over 500 Bm^3 gas reserves generated in the Cenomanian gas pool. Taking into account the vicinity of the North-Kamenomyssskoe, Semakovskoye and Tota-Yakhinsky fields explored in these waters, there will be constructed a new center for offshore gas production [20]. The map of the discoveries in the Barents-Kara region is given in the Figure 1.2.
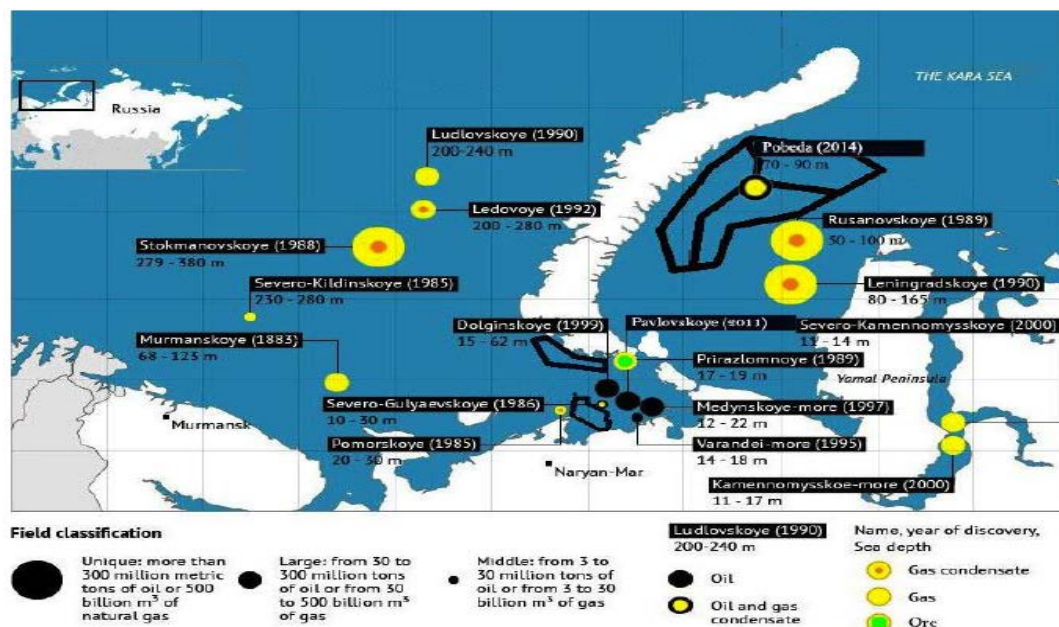
Figure 1.2. Russian Oil and Gas Fields in Barents - Kara region [45]

In 2014, as a result of a well drilling called Universitetskaya-1, «Rosneft» company discovered an oil-gas condensate field in the Kara Sea, which was called Pobeda. Official estimates show that

C1+C2 gas resorces make 130 MT and 395.6. Bm^3 of gas. These discoveries of gas were found in the Cenomanian and Apt-Alba Cretaceous deposits. The depth of the sea at the point of drilling is 81 m; the depth of the vertical well is 2113 m. The well was drilled under the conditions of open water in the 74 parallel north - 155.3 miles from the mainland territory of the Russian Federation. The result of drilling and gas and oil fields confirmed the prediction of high Cenomanian and Jurassic deposits prospectivity in the Kara Sea [20].

Recently «Gazprom» has conducted wide spatial explorations in the vicinity of the Yamal- Kara sea shelf.

In accordance with the obtained results, Mesozoic and Jurassic gas resource was detailed and confirmed as well as it had been done in the Rusanovskoye and Leningradskoye fields. The specifics of some fields in the Barents-Kara region are given in the Table 1.2.

Table 1.2. Specifics of some fields in the Barents-Kara region [27]

Parameter	Shtokmanovskoye	Ludlovskoye	Leningradskoye	Rusanovskoye	Pobeda
Gas trn m^3	3.8 (C1)	0.21 (C1+C2)	1.05 (C1+C2)	0.8 (C1+C2)	0.499 (C1+C2)
Condensate, MT	53.3 (C1)	-	3.0 (C1+C2)	7.8 (C1+C2)	-
Oil MT	-	-	-	-	-
Sea depth	280-380	280-380	80-165	50-100	70-90
Co-Ordinates	73.1 N, 44.1 E.	74.8 N 46.9 E	72.3 N 65.7 E	72.3 N 65.6 E	74.0 N 66.8 E
Operator	Gazprom	Gazprom	Gazprom	Gazprom	Rosneft

1.2. Laptev Sea

The Laptev Sea is one of the five polar seas of Russia. The shallow marine shelf with a depth up to 100 m represents the main part of the Laptev Sea.

The geological hydrocarbon resources, equal to 11.1 BT of oil equivalent with the density of 33 thousand tons/km^2, were used as baseline hydrocarbon saturation indicators of the Laptev Sea shelf. The oil and gas resources, most accessible for the development of the shelf zone, are estimated at 8.9 BT of oil equivalent with a liquid-gaseous HC ratio of 3:2. The geographical location of the Laptev Sea is shown in Figure 1.3 [20].

Figure 1.3. Geographic Location of Laptev Sea [44]

Eight of the detailed estimated areas of the offshore area vary from the point of view of recoverable resources in the range of values of 87–1552 MT of oil equivalent with their 80% concentration in the Oligocene - Miocene sediments of the shelf. At three sites - Lazarevskoye, UstLenskoye and Ust-Olenekskoe, the discovery of large deposits is predicted [29].

In order to assess the prospects for hydrocarbon saturation in the northwestern part of the Laptev Sea, a number of seismic exploration works using the methods of reflected waves, gravity, magnetometric prospecting of 16×16 km over an area of 32.6 thousand km^2 had been performed as a result of research of JSC «Marine Arctic Exploration Expedition ». As a result, new data were obtained on the structure of the previously practically unexplored region of the Laptev Sea shelf and adjacent structures of the Arctic Ocean [29].

Forecast resources of the sedimentary cover category D2 is 4 BT of fuel equivalent, recoverable resources is 2.7 BT of fuel equivalent. On the operations area, 17 local elevations have been mapped, the resources of which are estimated at 1.4 BT of fuel equivalent. Among local facilities, the most promising are structures correlated with the Olginsky oil bank with localized hydrocarbon resources of 1.2 BT of fuel equivalent [29].

1.3. East Siberian Sea

The East Siberian Sea is fundamentally different from all offshore seas of the Arctic Ocean. At the forefront, this difference lies in the most severe ice conditions. In this regard, the exploration and development possibility of oil and gas resources in the offshore area of the East Siberian Sea is significantly difficult. The geographical location of the East Siberian Sea is shown in Figure 1.4

Figure 1.4. Geographic Location of East-Siberian Sea [44]

The main prospects for hydrocarbon saturation of the East Siberian Sea are connected with the East Arctic petroleum province. Based on the phase assessment of forecast resources, it is assumed that most of the fields have a mixed (oil and gas) composition [20].

Taking into account the the sedimentary cover distribution in the province, its structural plan and tectonotypes, as well as analogies with the Sverdrup oil and gas reference basins, the northern continental slope of Alaska and the Chukchi Sea, the areas with optimal hydrocarbon resources are identified in which the main prospects are associated with the Upper Triassic-Lower Cretaceous complex. The productivity of the complex is confirmed by the discovery of deposits on the northern continental slope of Alaska and in the Sverdrup basin. The area of the plots is about 7% of the offshore area of the Eastern Arctic petroleum province; the overall amount of geological resources is 5,198 MT of oil equivalent, density is from 60 to 100 thousand tons/km^2 [20].

According to FSBI « All-Russian Research Geological Oil Institute», the resources of the East Siberian Sea are estimated at 4 BT of fuel equivalent. According to estimates by «Rosneft», the recoverable oil reserves on the East Siberian Sea shelf are 3,750 MT, and 1780 Bm^3 of gas [20].

1.4. Chukchi Sea

The Chukchi Sea is one of the marginal seas of the Arctic Ocean off the coast of Asia and North America. It washes the northern shores of the Chukchi Peninsula and the northwestern shores of

Alaska. In the west, the Chukchi Sea is connected to the East Siberian Sea by the Long Strait, in the south with the Bering Sea by the Bering Strait shown in the Figure 1.5.

Figure 1.5. Geographic Location of Chukchi Sea [44]

Large promising oil and gas resources are distinguished in the offshore area of North Chukchi basin. According to «All-Russia Petroleum Research Exploration Institute», the forecast resources of hydrocarbons in this basin are 2,354– 4400 MT of standard fuel.

The total resources of the oil and gas systems of the North Chukchi Trough, according to the estimate of «Dalmorneftegeofizika» company, are accounted for 2,510-3,140 MT (an average of 2,818 MT). Resources are unevenly distributed. The average density of resources for North Chukchi Trough is 45–55 thousand tons/km^2 that coincides with the density established for the Upper Permian-Lower Cretaceous system. The structures of the carbon-middle Jurassic and Upper Jurassic-Cretaceous systems are considered as promising objects [20].

Thus, the gas potential of the Arctic seas of Russia is most studied in the Barents-Kara region, where large and unique gas condensate fields are discovered. Gas reserves and potential resources are concentrated in bottom sediments of the Cenoman-Alb-Apt complex in the Kara Sea and Jurassic sediments in the Barents Sea. Taking into account the technical and economic indicators of the development, the gas resources on the Kara Sea shelf, including the deposits of the Ob and Tar Bays, are most available.

2. Analysis of the Potential Conditions for the Construction of Subsea Pipelines in the Arctic

2.1. General Environmental Conditions

The climatic features of the northern seas of Russia are determined by their geographical location, the impact of the cold Arctic and warm Atlantic Pacific basins, on the one hand, and the mainland of Eurasia, on the other. The high latitude position of the shelves determines the presence of a long (from 40 to 100 days a year) polar night [8].

Extreme temperatures can reach very high values. In winter, absolute fluctuations in the northern part of the Atlantic region and in the northern coast of Chukotka and Alaska range from -45 °C to +10 °C, and in the Siberian region of the Arctic from -55 °C (in some cases -63°C) to 0° (in some places to +4 °C) . In summer, absolute temperature fluctuations are less above the continental areas and adjacent offshore area from +32 °C to -6 °C, and in the southern parts of the seas the air temperature rises, and above the narrow coastal strip it increases very sharply [8].

Repeatability and precipitation vary significantly in different areas of the Arctic. Days with precipitation of 0.1 mm are most distinguished in the Atlantic region, slightly less in the polar region and the least in the north of Eastern Siberia. The annual amount of precipitation is distributed in a similar way.

Wind speed in the Atlantic and Pacific regions of the Arctic reaches an average of 6 – 8 m/s in winter and decreases to 4 – 5 m/s in summer. The reverse annual variation of speeds (from 2 – 3 m/s in winter to 4 – 5 m/s in summer) is noted in the Eastern Siberia regions [8].

The offset nature of water motions with a predominance of the northeastern general transfer is essential for the coastal region of the Arctic seas. The velocities of the total currents are 20 – 60 cm/s, however, the maximum values can exceed 100 cm/s. Wind and tidal currents have the greatest impact [8].

As a consequence of tidal oscillations, the total semidiurnal sea-level changes are dominated on the shelf. The average value of tidal changes in the level is 0.2 – 0.3 m in the East Siberian sea, in the Barents and Kara seas it's 0.5 – 0.7 m. The total changes in the level during storm surges can be from 2 to 5 m. Annual oscillation in the sea level are slight – it can be from 8 to 16 cm [8].

Wind waves are especially developed during the period when there is no ice cover or with its small cohesion. The most developed and highest wind waves occur in the Barents Sea. In general, wave heights of 3 – 9 m, most often observed in the fall, are typical for the offshore area of the Arctic seas. The calculated wave heights possible every 50 or 100 years, can reach 14 m or more. The average speeds of wind currents for different seas vary from 2 cm/s (Laptev Sea) to 40 – 50 cm/s (Chukchi Sea), but the maximum speeds of the total current can be much higher [8].

In winter, in the shallow waters, water masses from the surface to the bottom have a negative temperature, dropping at the bottom to -1.5 °C, only in the furrow of the Kara Sea, in the deep-water part of the Laptev Sea, their temperature is positive and reaches 1 – 1.5 °C. Summer processes develop actively in a relatively narrow coastal region releasing from ice for 2 – 3 months. Only a thin surface layer of water is warmed up. At depths of more than 25 – 30 m, the water constantly has a negative temperature; the waters are heated only in individual bays and in some other limited areas of the coastal zone of the Arctic basin to +12 °C, and the warming extends only to a depth of 30 – 75 m [8].

According to [8], within the Arctic basin, four main and two intermediate water masses are distinguished:

The surface arctic water mass is characterized by a year-round negative temperature, a salinity of 29 – 33.5 ‰, and an average layer thickness of 25 – 50 m. The movement speed of the arctic water mass is 1.1 – 2.3 cm/s, in some places it increases to 7.2 cm/s.

The deep-water Atlantic water mass is separated from the upper to the underlying water masses by intermediate ones. It enters the Arctic basin from the Atlantic Ocean and accounts for 42% of the heat flow of the Arctic basin, penetrating only into the western seas. At the entrance to the Arctic basin, the Atlantic waters have a temperature of +8 – +14 °C, and in the area of the Franz - Joseph Land, it drops to + 2 °C. The salinity of the waters is 34.9 – 35.6 ‰. The thickness of the Atlantic water mass in the Eurasian sub-basin is 300 – 400 m. The bulk of the water moves in the direction opposite to the movement of the Arctic waters, has branches in the Barents, Kara Sea and, to a lesser extent, in the Laptev Sea.

Pacific warm water mass of 30 – 75 m thickness is located in the eastern part under the surface of the Arctic water. The maximum water temperature is +4 °C, salinity 32 – 33 ‰. The general direction of movement of this water mass is through the Bering Strait along the Canadian Arctic archipelago, with a branch into the Chukchi Sea.

Bottom water mass from a depth of more than 800 m fills deep-sea oceanic hollows; their thickness varies depending on the depth of the ocean. The bottom water temperature is from -0.4 to -0.9 °C, salinity is about 35 ‰.

One of the main features of the Arctic region is permafrost, which extends to the shelf area. Almost everywhere, perennially cooled rocks with negative temperatures represent the cryolithozone. The most studied are the permafrost conditions of the Barents and Kara seas.

The coastal region of the seas includes the permafrost soils, which contain highly mineralized waters (cryopeg water). The thickness of this layer is from several tens to several hundred meters. With increasing distance from the coastline, the permafrost thickness decreases and in the seaward areas of the shelf they are present as inclusions in the perennial cooled rocks.

Bottom permafrost soils are characterized by high salinity, which determines their high corrosive activity. Large stocks of ice determine the ability of soils to large deformations during thawing

The Arctic offshore seas, with the exception of the western (near Atlantic) part of the Barents Sea, the eastern (near-Ocean) part of the Chukchi Sea and the mouth areas of large rivers, have negative bottom temperatures, reaching minus $1.5 – 2.0$ °C. Thus, there are sufficient conditions for the presence and preservation of permafrost under the seas [8].

The widespread permafrost in the coastal shelf zone of the Arctic causes a number of specific features of the geological environment associated with the development of cryogenic physical and geological processes that can have a direct impact on construction. These are thermokarst, thermal erosion, cryogenic swelling, cryogenic cracking, icing, and new formation of permafrost. The occurrence of large inclusions of ice (permafrost) close to the seabed may cause emergency situations during anthropogenic (human) impact on the geological environment. A summarized description of the conditions for the construction of offshore pipelines in the Arctic seas is presented in Table 2.1.

Table 2.1. General information of environmental conditions of Russian Arctic seas

	Barents Sea	Kara Sea	Laptev Sea	East-Siberian Sea	Chukchi Sea
Temperature	Summer up to + 10 ° C (+ 30 °C) Winter to -20 ° C (-40 ° C)	Summer up to + 8 ° C (+ 28 ° C) Winter to -30 ° C (-52 ° C)	Summer up to + 8 ° C (+ 28 ° C) Winter to -32 ° C (-52 ° C)	Summer up to + 6 ° C (+ 28 ° C) Winter to -32 ° C (-52 ° C)	Summer up to + 6 ° C (+ 28 ° C) Winter to -30 °C (-48 ° C)
Ice	The western part never freezes. May - the greatest distribution of ice	From October to July, completely ice covered	From November to July completely under the ice, height of hummocks up to 20m	From September to July completely ice covered	December to June, completely ice covered
Winds	8-16 m/s (wind gusts up to 40 m/ s)	8-16 m/s (wind gusts up to 40 m/ s)	4-8 m/s (wind gusts up to 38 m/ s)	5-8 m/s (wind gusts up to 38 m/ s)	6-10 m/s (wind gusts up to 46 m/ s)
Depths	average 200m (max 600m)	average 50m (max 600m)	Average up to 50m (max 3385m)	average 4m (max 155m)	average 77m (max 200m)
Currents	10-25 m/s	5-10 m/s	2-5 m/s	0,5-5 m/s	2-5 m/s
Grey sky	80% of the year	65% of the year	40% of the year	40% of the year	40% of the year
Amount of precipitation	Up to 865 mm per year	Up to 390 mm per year	Up to 350 mm per year	Up to 200 mm per year	Up to 480 mm per year
Average shelf length	200 km	260 km	130 km	600 km	500 km

2.2. Ice Conditions

The planning of the construction of underwater pipelines mainly depends on the ice regime of the construction site. This section describes the generalized characteristics of the ice conditions in the Arctic region.

According to [8], in the Arctic seas for about eight months (from October - November through May - June), ice formation and growth processes occur. In winter, all the seas are completely covered with ice of various thickness, with a cohesion of 9 – 10 points. In the coastal shallow areas the formation of fast ice occurs at different times from mid-September to early December. At the end of August, steady ice formation begins in the north of the seas. In the first decade of September, young ice appears on the northern borders of the Kara and Laptev seas, and by the end of the

second decade of September in the north of the Chukchi Sea. On average, the Laptev and East-Siberian seas completely freeze for 35 – 40 days. The Kara and Chukchi seas freeze for 80 – 85 days. The perennial amplitudes of the periods of sustainable ice formation in the Arctic seas vary from 30 to 90 days. The ice covers the Arctic seas for more than 300 days a year, making them essentially a solid ice field [8].

After a steady ice formation, an increase in ice cover occurs. From October to November, the growth rate of ice increases, in November, this process proceeds with maximum speed (an average of 12 cm per decade), then, as the thickness of the ice increases, the growth process slows down and in May the ice increases by an average of 2 cm per decade. By the end of the growth period, the greatest thicknesses of the flat ice of the autumn formation are observed in the Laptev and East Siberian seas - 190–220 cm, the smallest in the southwestern part of the Kara Sea - 100—130 cm, slightly larger, up to 160 cm in the southwestern part Chukchi Sea [8].

Drifting ice is located beyond the sea boundary of fast ice. In the Kara and Laptev seas in the autumn-winter period, drift is directed to the northwest-north and is accompanied by the removal of ice into the Arctic basin. In the East Siberian Sea, ice drifts has a direction from west to northwest. Therefore, the removal of ice from the sea to the Arctic basin is weakened and the formation of ice lead is difficult. During the entire cold period in the Chukchi Sea ice drift is directed towards the coast and as a result, ice from the Arctic Basin enters the sea [8].

First-year ice prevails in the Arctic seas. Biennial and perennial ices in the form of spurs of oceanic ice masses are most often observed in the East Siberian Sea, in the north of the Laptev and Kara seas.

Melting of ice begins at different times and occurs at the end of May-second decade of June. With the beginning of thawing, under the influence of dynamic processes, zones of open water, discontinuous ice appears. Ice with cohesion of 7 – 10 points are localized in ice massives. The ice clearing of the Arctic seas is most intense during August and terminates at the end of September. On average, before the start of ice formation, the southwestern part of the Kara Sea (95%) is almost completely free of ice (95%), the eastern part of the Laptev Sea is 80—85% free. The northeastern part of the Kara Sea and the western parts of the Laptev and East Siberian seas are cleared by 50%. On average, the eastern part of the East Siberian Sea is cleared of ice by only 27% by the end of the period [8].

In winter, ice covers almost the entire area of the Arctic, and in summer, it covers about half. Only the very south of the Barents Sea, where the Gulf Stream flows, does not freeze all year round, but strong northern winds here raise waves up to 20 m in high [8].

Drifting ice throughout the year are in continuous motion under the influence of currents and winds. Perennial drifting ice has a significant thickness, changing cohesion and covers almost the entire Arctic Ocean, including the shelf seas of the Arctic. [8].

Thus, based on the analysis of statistical meteorological data applied to the conditions of the Arctic seas, approximate work schedules for the construction of underwater pipelines are suggested and presented in Table 2.2.

Table 2.2. Planning of the construction time for offshore pipelines in terms of ice factor

Month / Sea	January				February				March				April				May				June				July				August				September				October				November				December			
	1	2	3	4	1	2	3	4	1	2	3	4	1	2	3	4	1	2	3	4	1	2	3	4	1	2	3	4	1	2	3	4	1	2	3	4	1	2	3	4	1	2	3	4	1	2	3	4
Barents Sea (West)																																																	
Barents Sea (East)																																																	
Kara Sea																																																	
Laptev Sea																																																	
East Siberian Sea																																																	
Chukchi Sea																																																	

—————— Continuous ice

------------------ Open water

—·—·—·— Variable time

☐ Downtime for meteorological reasons

Thus, the Arctic seas of Russia are characterized by harsh climate, low ambient temperature, seasonal ice cover, drifting icebergs, high storm waves. All these factors are need to be dealt with a whole range of works in the construction and operation of subsea pipelines in the Arctic. The conditions of each region should be taken into account in the case of pipeline design.

3. Analysis of the Current State of Offshore Pipeline Construction in the Arctic

Development of the arctic and subarctic shelf in the USA and in Canada was performed at high speed from the 60s. That time the industrial development of Alaska began, when in the arctic part of Alaska large offshore gas and oil fields were found, which required the construction of offshore pipelines transportation system [8]. There are also Russian subsea pipeline construction projects in the Arctic and subarctic regions. The Table 3.1 shows the implemented subsea pipelines construction projects in the Arctic and subarctic regions.

Table 3.1. Existing projects of pipeline construction in the Arctic and subarctic regions

Project	Location
Drake (1978)	Canadian Arctic Archipelago (Canada)
Northstar (2000)	Beaufort Sea (USA)
Ooguruk (2007)	Beaufort Sea (USA)
Nikaitchuq (2011)	Beaufort Sea (USA)
Sakhalin-1 (2005)	Sea of Okhotsk (Russia)
Sakhalin-2 (2003)	Sea of Okhotsk (Russia)
Kashagan (2007)	North Caspian (Kazakhstan)
Varandey oil export terminal (2008)	Pechora Sea (Russia)
Baydaratskaya Bay pipeline crossing (2007)	Kara Sea (Russia)

3.1. «Drake» Project

In April 1978 the construction of the first subsea pipeline under the ice in the arctic region of Canada in the gas field Drake-Point was finished. The pipeline, consisting of the casing 610 mm (24 inch) in diameter, which has several pipes of a smaller diameter, is the flow line, connecting the subsea gas well with the land facilities. The pipeline was assembled on the shore and dragged over the bottom of the subsea trench with the winch, set up on the ice. A winch cable went through the slot in ice to the head of the pipeline.

The project excluded the necessity of using divers. Special plough was used to make the subsea trench. When the 1.2 km pipeline was assembled, its annular space was filled with nitrogen.

A concept «pipe inside a pipe» was used for coolant feeding, in order to exclude permafrost soil melting. The shore approach was built by horizontal directional drilling and the offshore part was trenched by 1.5 meters [8]. The Figure 3.1 shows the cross-sectional view of the pipeline used in the «Drake» project.

Figure 3.1. Cross-section of the Drake Project Pipeline [1]

3.2. «Northstar» Project

The projects of subsea pipelines construction in the Beaufort Sea, particularly the «Northstar», the «Ooguruk», the «Nikaitchuq» projects, are an example of the successful realization of the subsea pipelines construction in the Arctic. Exploration of arctic fields in these projects is carried out by artificial islands. Its products are being pumped to the onshore facilities through the trenched subsea pipelines.

All pipelines are located in the coastal area of the Beaufort Sea, at the Alaska North Slope. The maximum pipe diameter is up to 460 mm (18.1 inch), the water depth is up to 12 meters, the length is up to 10 km [7]. The Figure 3.2 shows the map of the pipelines in the Beaufort Sea.
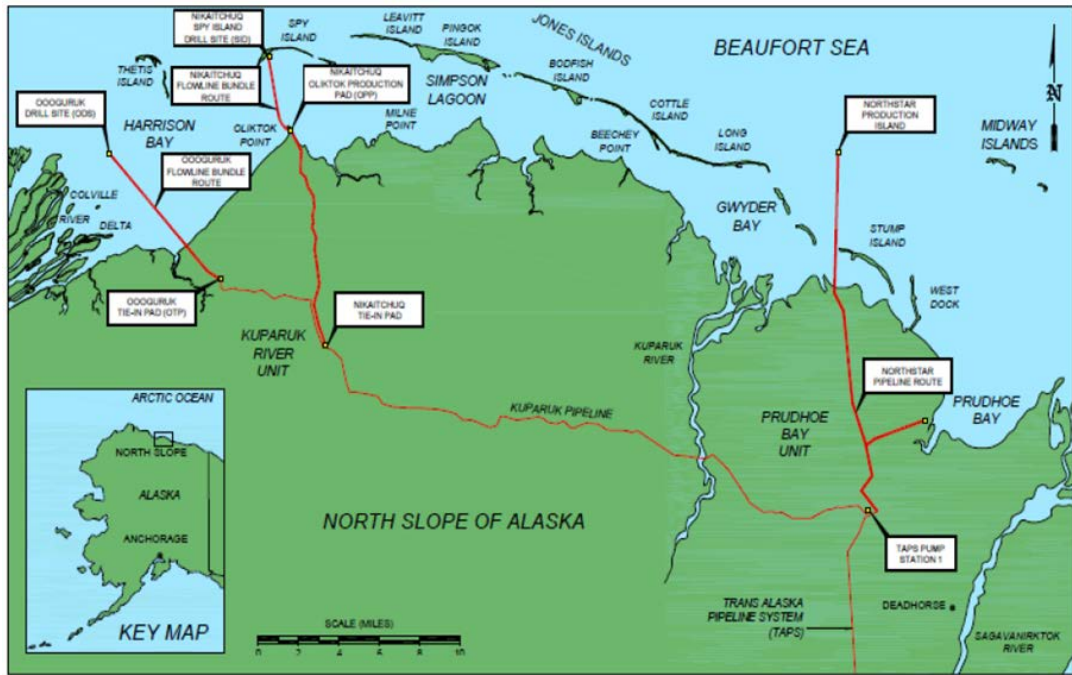
Figure 3.2. The map of the «Northstar», the «Ooguruk» and the «Nikaitchuq» Pipelines [7]

The artificial island «Northstar» with an area of 20 thousand m^2 is located on the south of the Beaufort Sea, 9.7 km to the north from Alaska coast and 19 km to the north-west from Prudhoe Bay. The island was created for the development of the oil basin «Northstar», situated 3800 m deeper the sea bottom.

The «Northstar» island was the first project in the Beaufort Sea where the subsea pipeline was used for oil transportation to the shore.

The pipeline bundle was installed in winter 2000 and consists of the two 10-inch gas and oil supply lines, and it also has lines for leak detection. Maximum designed depth of the burial is from 1.8 to 2.1 meters [7]. The cross-section of the «Northstar» pipeline is in the Figure 3.3
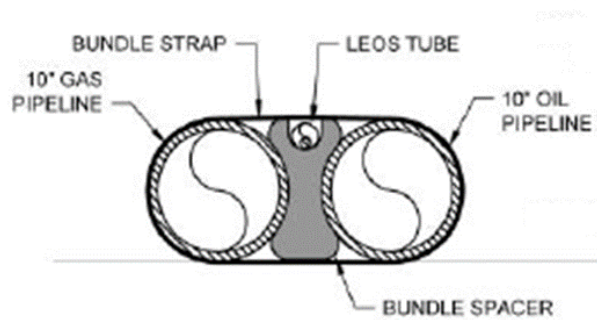
Figure 3.3. Cross-section of the «Northstar» Pipeline [7]

The «Northstar» pipelines were constructed from January till April 2000 using standard pipelaying equipment, installed on artificially thickened sea ice (Figure 3.4). The ice slot was made with the help of special excavator. The ground from the dug trenches was piled near the ice slot and was used for pipeline backfilling after its construction. No part of the «Northstar» pipeline was installed from a floating pipe-laying barge due to shallow depth of the sea [7].

Figure 3.4. «Northstar» Pipeline Installation [7]

3.3. «Ooguruk» Project

The artificial island «Ooguruk» is located south-west of the Beaufort Sea, approximately 5 miles away from the coast, and connected to the coastal equipment with 12x16 inch subsea pipeline bundle as «pipe in pipe», which consists of 8-inch isolated water injection line, 6-inch gas source transportation and 2-inch fuel feed line for heating purposes. The cross-section of the «Ooguruk» pipeline is in the Figure 3.5 [7].
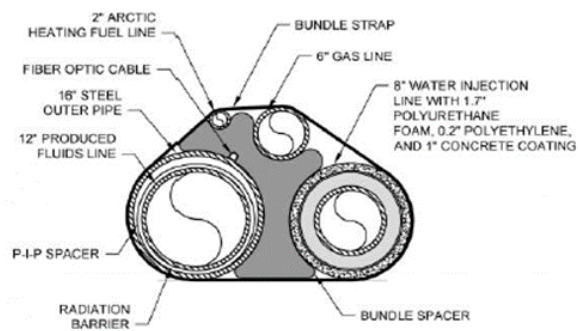
Figure 3.5. Cross-section of the «Ooguruk» Pipeline [7]

The «Ooguruk» pipeline was constructed in January-April 2007 using the standard equipment on the artificially thickened ice, the same as in the «Northstar» project.

3.4. «Nikaitchuq» Project

The artificial island «Nikaitchuq» is connected to coastal facilities: 14x18-inch subsea bundle as «pipe in pipe», consisting of 12-inch isolated water injection line and 2x4 inch fuel feed line for heating purposes. The cross-section of the pipeline is in the Figure 3.6.
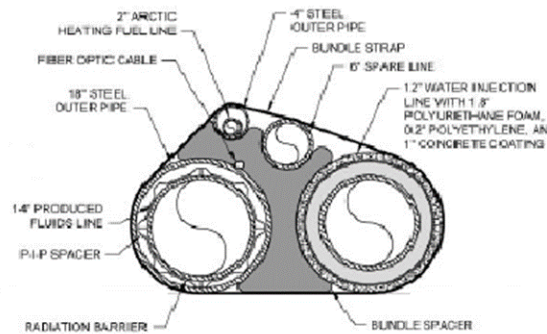
Figure 3.6. Cross-section of the «Nikaitchuq» Pipeline [7]

The subsea «Nikaitchuq» pipeline bundle were constructed from the surface of winter sea ice as in the «Northstar» and «Ooguruk» projects. The ice was artificially thickened along the route. The surface of ice was also used for temporary storage of soil, left from the trenches [7].

3.5. «Sakhalin-2» Project

The project includes the development of two offshore fields: Piltun-Astokhskoye (mainly oil field with associated gas), Lunskoye (mainly gas field with associated gas condensate and oil fringe).

Subsea pipelines of total length approximately 270 km connect producing platforms on Piltun-Astokhskoye field «PA-A», «PA-B» and Lunskoye field «Lunskaya-A» with onshore oil and gas pipeline systems, leading to the LNG plant on the south of Sakhalin.

Crude oil and dry gas are transported through 14-inch concrete subsea pipeline from the platforms «PA-A» and «PA-B» to a landfall collecting pipe, located in the village Chaivo at distance of 46 and 71 km, respectively, with total length 234 km [9].

Two subsea condensate flow lines with diameter of 30 inches were built to transport unstabilized condensate from the platform of Lunskoye field to the onshore facilities. The length of each condensate flow line is 15 km. The pipeline system includes a power cable and a communication cable, and 4.5 inch (114.3 mm) monoethylene glycol (MEG) feed line [9]. The pipeline map of the «Sakhalin-2» project is in the Figure 3.7.
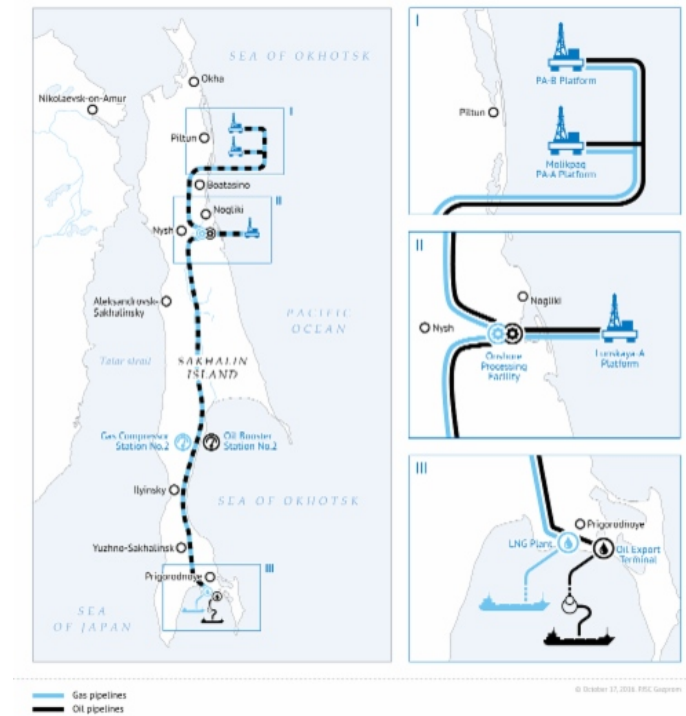
Figure 3.7. The Pipeline Map of the «Sakhalin-2» Project [39]

The construction of the pipelines considers requirements to high strain capacity and extreme temperatures of the environment, in order to exclude possibility of brittle fracture. The pipelines were installed from a pipe-laying barge «Seamac», shown in the Figure 3.8 [9].

Figure 3.8. Pipe-laying Barge «Seamac» [9]

3.6. «Kashagan» Project

Kashagan is an oil field in Kazakhstan, located in the north of the Caspian Sea. Kashagan field development will be carried out in several steps. Currently the work is on the stage of pilot development planning (PDP). At this stage the plan is to extract 370 thousand barrels of oil per day (13 mln tonnes a year). PDP is followed by the next stages of the development, which are at the stage of planning at the moment. In aggregate, all stages are full-field development. Field facilities construction is performed on artificial islands [41].

The northern part of the Caspian Sea is characterized by the existence or seasonal ice-cover, which can be up to 0.4 m thick. Subsea pipeline system installation for the «Kashagan» project in the North Caspian began in 2007 and eventually will include hundreds of kilometres of buried pipelines from 8 (203.2 mm) to 28 (711.2 mm) inches in diameter [9]. Field facilities scheme of the Kashagan field is presented in the Figure 3.9.
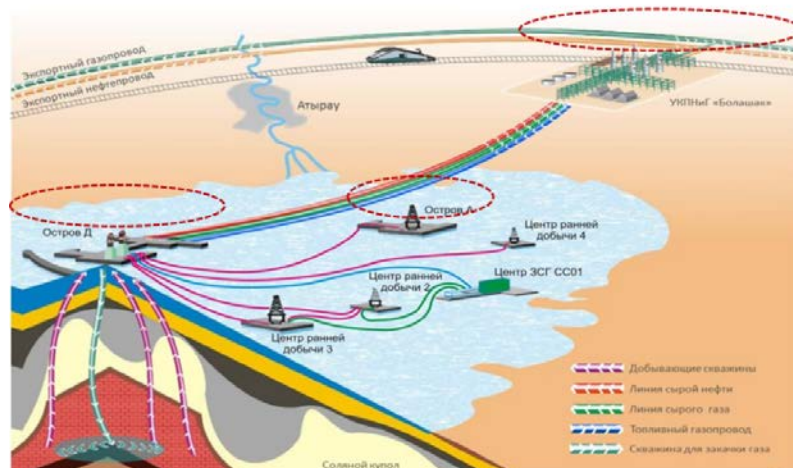
Figure 3.9. Kashagan Field Facilities Scheme [41]

Sea depth does not exceed 7 meters. The pipelines were trenched with the use of standard pipelaying equipment, installed on the ice. The ice slot was made with the help of backhoe dredges, in a similar way to American pipelines in the Beaufort Sea. The depth of the pipeline trenches does not exceed 2 meters.

3.7. Varandey Oil Export Terminal

Varandey oil export terminal is a fixed offshore ice-resistant off-loading terminal (FOIROT). Its aim is to export oil, extracted by the oil company «Lukoil» and other oil companies in Timan-Pechora basin, on shipping routes. FOIROT is shown in the Figure 3.10.

It was put into operation in June 2008. The terminal was installed at a depth of 17 meters in the Barents Sea, 22 km away from the coast in the Varandey village of the Nenets Autonomous region. The ice season of the region lasts 247 days. The sheet ice thickness reaches 1.8 m [37].

Figure 3.10 Varandey Oil Export Terminal [38]

From the terminal oil is transported by shuttle tankers to the port Murmansk to the storage «Kola» for the following export. The terminal operates throughout the year. Ice-breaking ships operate during winter.

The terminal is connected to onshore oil storage by the two 36-inch pipelines with a length of 22.6 km. Steel of the pipelines is X65. The thickness of concrete weight coating is 70 mm; the depth of the burial is up to 2 meters. Maximum depth along the pipeline route is 23 meters [37].

3.8. Baydaratskaya Bay pipeline Crossing

The pipeline crossing through the Baydaratskaya Bay is a part of the Yamal-Europe gas pipeline, which is intended to supply natural gas from the Yamal Peninsula fields, (namely Bovanenkovskoe and Kharasavey) to the gas transmission network of the Central part of Russia and further to

Western Europe. The geographical location of the underwater crossing of the pipeline through the Baydaratskaya Bay is presented in Figure 3.11.

As part of this project, a large-diameter underwater gas trunkline (1219 mm, wall thickness 27 mm, steel X65) was built in the Arctic shelf of Baydaratskaya bay water area, in the Kara Sea. The Baydaratskaya Bay water area is located between the Yugorsky Peninsula and the Yamal Peninsula. The length of the offshore part of the pipeline is 70.6 km; the thickness of the concrete coating is 85 mm [37].
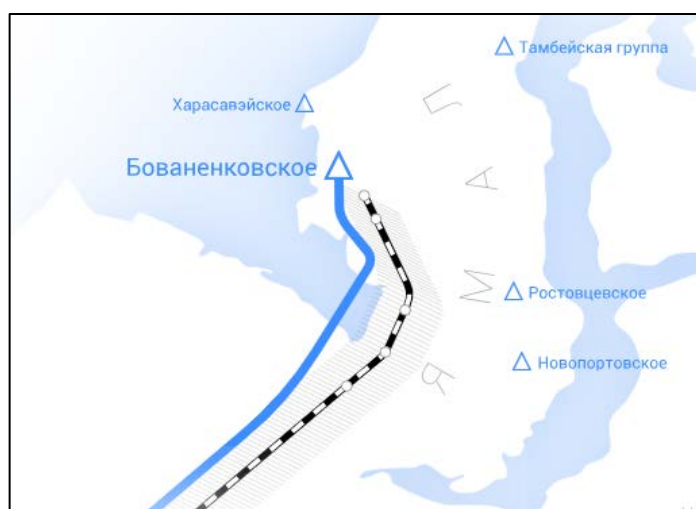
Figure 3.11. Baydaratskaya Bay Pipeline Crossing [39]

The conditions of construction are characterized by a harsh arctic climate with a large annual temperature amplitude, frequent storms with wave heights of up to 6-8 meters, snowstorms and high relative humidity throughout the year, a distant location from large settlements, a short (3 months) period of navigation .

From the analysis, we can draw the following conclusions. Today there are a small number of offshore pipeline construction projects in the Arctic. When constructing future pipelines in the Arctic, such factors as the possibility of ice gouging, the almost ubiquitous distribution of permafrost soils, a limited period of open water, as well as increased environmental requirements for the Arctic region need to be taken into account.

4. Features of Construction and Operation of Underwater Pipelines in the Arctic shelf

Shelf location sets external conditions under which underwater pipeline fitting and operation are carried out. Moreover, their impact differs according to the work being done. These conditions determine the choice of materials and the design of a pipeline, flow charts and methods of construction, machines and mechanisms. Considerable differences in the conditions of separate shelf areas require an individual approach to assessment of their impact on the construction.

There is a number of unique factors in the construction and operation of Arctic subsea pipelines that differ from conventional subsea pipelines expatriated under the conditions of open water, which will be described below.

4.1. Ice Gouging

Ice gouging occurs in a coastal zone for most Northern continents. Sea ice in the Arctic is driven by winds and currents and tends to develop into ridges. It mainly happens during freeze-up in autumn and ice break in spring, when the ice sheet is floating. These ice ridges have underwater keels that move together with the ice cover. In other regions glacial ice in the form of iceberg can have an underwater part exceeding 100 m. Sometimes such keel penetrates into water, the depth of which is less than the one of keel draft, and gouges furrows in a seabed. The most common way to protect pipelines against damage by ice keel under the conditions of ice gouge is embedding into a trench to a chosen depth below seabed [19]. The process of ice gouge is shown in Figure 4.1.

Figure 4.1. Ice Gouging Process [19]

To measure the depth and width of separate furrows left by ice, geophysical investigation of the seabed and high-resolution bathymetric data collection are carried out. To detect separate furrows and measure their orientation, side-scan sonar recordings are used. Furrows on the seabed are modified under the influence of repeated gouging, sedimentation, and displacement of bed loads by bottom currents. In shallow-water zones with sandy deposits exposed by powerful waves and currents during open water season, all traces of the ice gouge can be destructed by the end of every summer season [18].

The pipeline lying on the seabed may not withstand the interaction with ice keel. As a rule, the trenching below the projected level of seabed gouging is required. When the ice keel is in contact with any point of the seabed at the level of keel bottom, vertical and side efforts start to affect the soil. This results in vertical and side displacement of the soil below the keel depth which is usually termed as "under trench deformation" of the seabed. This deformation can trigger the impact of efforts on the pipe body and lead to the pipeline deformation. Pipeline configuration after gouging and bending deformation depends on pipeline properties, soil characteristics, rated depth of ice gouge, and depth of the pipeline location below the seabed. To reduce pipeline deformation to acceptable limits, it must be placed in the trench at a sufficient depth below the ice keel. If the pipeline is placed below the zone of considerable soil movement, it will be under increased pressure but slight bending deformations in view of relatively small soil movement. If the pipeline is placed within the zone of considerable soil movement, it may be subjected to excessive plastic deformation. It is therefore necessary to carry out an assessment and calculate soil displacement at the depth of pipeline laying under the influence of ice gouge as well as resulting bending deformation [18].

4.2. Strudel Scour

Strudel scour - Strudel in translation from German means "whirlpool". This effect occurs when a large amount of fresh water during the spring melting season flows onto the ice cover and drains through small openings or cracks in the ice creating a whirlpool. This results in a zone of increased pressure that can lead to sea floor scour, creating a hollow more than 3 meters deep. These phenomena usually occur at a depth from 2 up to 8 meters in a maritime area near river deltas. The deepest scours occur in shallow water (i.e. at a depth from 2 up to 3 meters), where the power of water pressure is enough to wash away sea floor sediments directly under the ice [19]. The process of strudel scour is shown in the Figure 4.2.
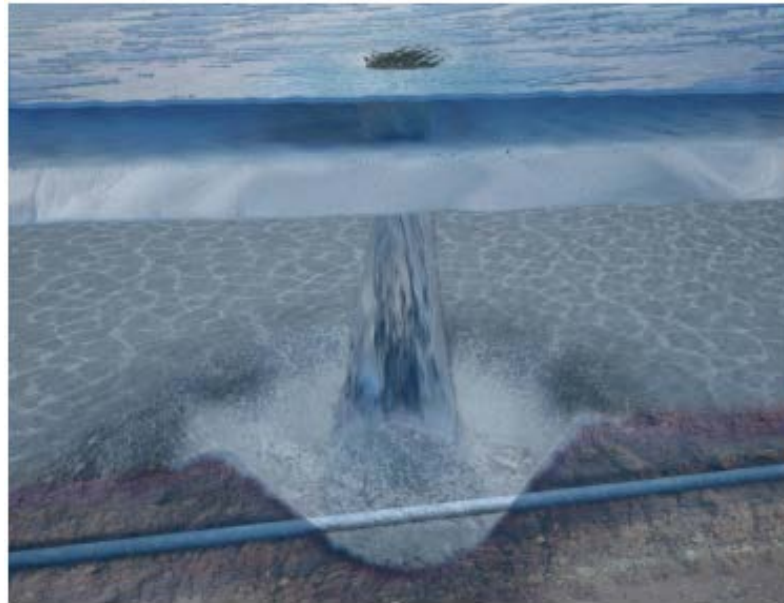
Figure 4.2. Strudel Scour [19]

If the seabed scour occurs above the trenched pipeline, it can lead to uncovering of pipeline and formation of free span. Under extreme conditions, an uncovering part of the pipeline may be subjected to hydrodynamic loads from currents as well as the vortex induced vibrations.

4.3. Presence of Permafrost Soil

Permafrost soils are prevalent in the Arctic regions of the Russian Federation. Spreading of permafrost can be continuous to a depth of hundreds of meters from the surface or it can be discontinuous as separate lenses. Permafrost is very sensitive to temperature changes. During the pipeline operation under the influence of high temperature of the pumped product, the surrounding soil warms up and as a result permafrost starts to melt. Permafrost soils that used to be a reliable bottom turn into slush over several summer seasons. There pipelines may come to the surface and their transverse displacement and deformation may occur [19]. Permafrost soil thawing near the pipeline is shown in the Figure 4.3.

The probability of pipeline bending due to permafrost thawing along the pipeline route depends on such main factors as the size of voids, soil type as well as ice and moisture content in the formation. This phenomenon may be exacerbated by water migration to the freezing zone with subsequent forming of ice lenses [19].

Figure 4.3. Permafrost Thawing Near the Pipeline [19]

To prevent this phenomenon, the pipeline must be thermally insulated. It is necessary to monitor the pipeline temperature and permafrost soil surrounding it.

4.4. Upheaval Buckling

In case of the subsea pipeline operation at the temperature (and pressure) above the temperature of pipeline construction, thermal expansion of the pipeline may occur. Since the trenched pipeline is bounded on all sides by the surrounding soil, axial compression force occurs. If the underground pipeline has a residual vertical deformation, for example, caused by a rough surface of the trench bottom formed during the construction, axial force will cause pipeline turn-up in a vertical plane. It is possible in case the vertical force caused by pipe buckling exceeds the downward force, namely the pipe's own weight in a submerged state, the resistance force of the overlying soil [19]. The mechanism of forming of the pipeline upheaval buckling is shown in the Figure 4.4.
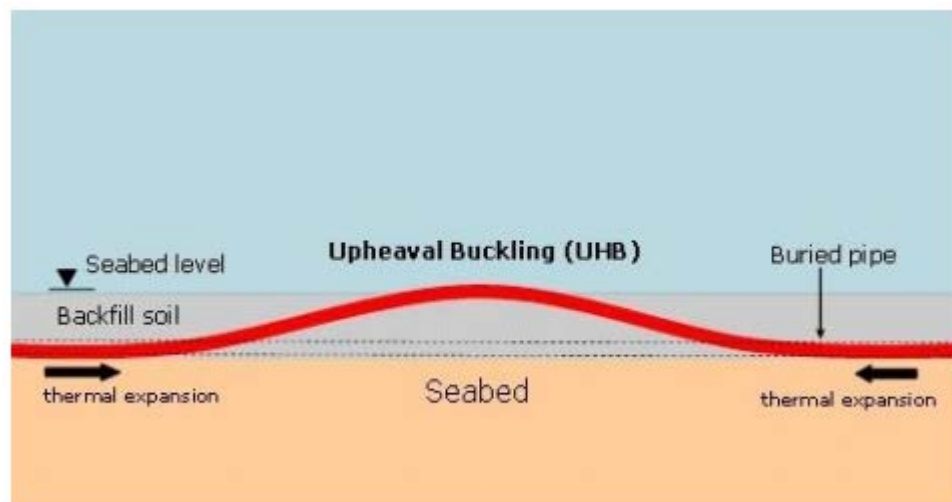
Figure 4.4. Pipeline Upheaval Buckling [30]

36

This phenomenon is typical for subsea pipelines. Despite the fact that this phenomenon is not unique for the Arctic conditions, pipelines in the Arctic are usually laid at a lower ambient temperature and, consequently, are subjected to greater temperature fluctuations during operation. Furthermore, permafrost soil bulging may cause local deformation in the pipeline, which may further lead to the pipeline upheaval buckling [19].

The analysis of the possible pipeline upheaval buckling is carried out in order to determine the minimum thickness of the soil protective coating, which has to provide the necessary resistance in order for the pipeline to remain in the initial position.

4.5. Pipeline integrity monitoring

Real-time monitoring of pipeline integrity is a system for monitoring the pipeline state using different sensors aimed at increasing pipelines productivity. The aim of pipeline integrity monitoring is to assess operating conditions, to increase the pipeline productivity and capacity, to prolong the service life as well as to alert the operator in case of the violation of the pipeline integrity [4].

Monitoring of the arctic pipelines state may be hampered due to such phenomena as ice gouge, strudel scour, pipeline cross bending, permafrost soil thawing around the pipeline, presence of the seasonal ice cover as well as remote location of pipeline systems. Visual inspection of pipelines using remotely operated vehicles (ROV) may be restricted due to the necessary pipelines trenching. All these factors determine the necessity to apply an integrated approach when monitoring the pipeline integrity in the conditions of the Arctic [4].

There are two main methods of monitoring underwater pipelines in the Arctic so far:

- − Internal control systems based on measurements of the flowrate, pressure, temperature, transient processes analysis, etc.
- − External control systems, in this case sensors are installed outside the pipeline.

These methods include control systems of mechanical impurities removal, corrosion, hydrogen sulfide content, pipeline wall thinning, monitoring of cracks, corrosion as well as free spanning pipelines control. Flow meters, scrapers, temperature and acoustical sensors, and optical fiber cables are used for these purposes [4].

One of the determining factors when controlling the pipeline integrity is leak monitoring. Because of the presence of the ice cover, leaks of smaller volumes ("chronic" leaks) may not be identified. This fact can lead to a potential accumulation of contamination volumes under the ice cover. High-precision optical fiber sensors have significant potential to address this problem [4].

4.6. Pipeline Shore Crossing Design for Arctic Subsea Pipelines

The shore crossing of subsea pipelines in the Arctic area can become a complicating task due to existence of permafrost found everywhere. Permafrost formation itself is a soil that acquired a maximum annual temperature below water-ice transition temperature. If composition of rock includes a significant amount of interstices filled with solid water (interstitial ice), there is a high probability of permafrost to be found unsteady. Interstitial ice melts as the temperature increases, at that there start to develop voids in the rock structure that can cause a rock fall. In addition, permafrost melting can be caused by a physical contact with pipeline system as pipes pump up the warm oil causing the temperature raise [5].

When given a permafrost conditions, it is usually considered to install a ground-surfaced pipeline propped up with a special supports. However, considering underwater pipeline construction, there is a transition part between offshore and onshore parts of pipeline which has to be designed in such a way to guarantee integrity of the shoreline and reduce accident probability.

While engineering the pipeline intersection of a shoreline in the Arctic shelf, one must consider following [32]:

- Intensive wave effect of the area;
- Shoreline erosion;
- Potential ice gouging impact;
- Human activity (trawl nets impact);
- Permafrost thawing;
- Ice ride up.

Nowadays there are several main ways to intersect a shoreline with underwater pipelines.

- Open cut trenching;
- Horizontal directional drilling method;
- Tunneling.

Open cut trenching can be carried out with three different ways [32]:

- Pipeline is assembled on the pipelaying barge and then is winched on to the shore by using a cable block placed on the shore;

- Pipeline is assembled on the piplelaying barge and then is winched on the shore using winches placed on the shore;

- Pipeline is assembled on the shore and then is winched to the sea by using a winch-equipped pipelaying barge.

The ways of how to lay a pipeline into prepared trench are shown in Figure 4.5.The selection of laying method depends on the depth of the inshore area and the installation method used to lay a main part of the pipeline.

cable block

Pipe string setting and winching using pipelay barge

winch

Shore winching

Winching using winched vessel
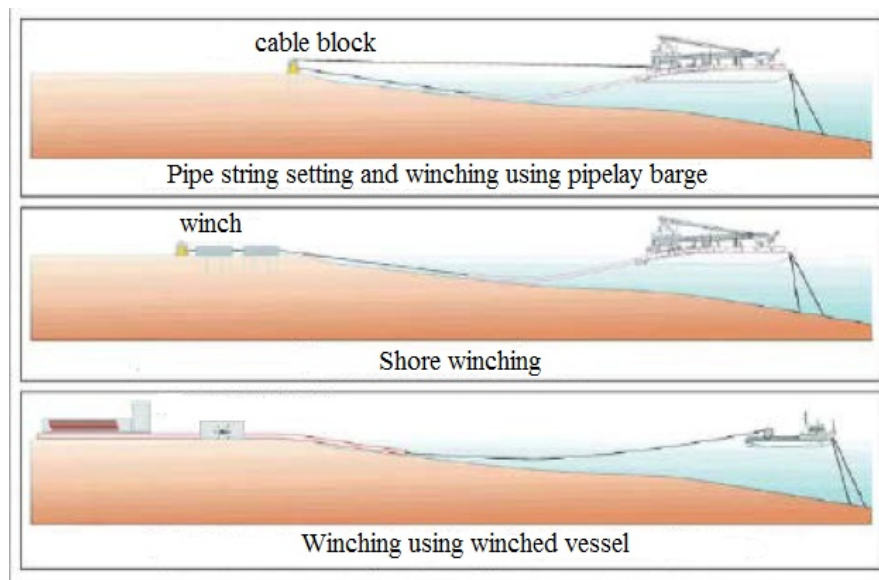
Figure 4.5. Pipeline Winching Methods [32]

Inshore and landfall wet section pipeline trenching can be employed in low angle inshore sections and such an area where the geological settings make it possible to perform groundworks. As a rule, a top line of a pipe is buried under 1.5 m of earth [32]. However, in the Arctic area this kind of method is rather troublesome due to permafrost soil, melting of which can cause deformation and breakdown of the pipeline.

The second way of shore crossing is horizontal directional drilling method (HDD). The HDD method is used when geological settings do not allow performing groundworks effectively. Using this method, it is possible to intersect both cliffed coast and the objects on it as well. There are two ways of shore crossing implying pipeline offshore landfall and pipeline onshore landfall with the following development of surface trench on the shoreline. With that in mind, there are 4 main ways

depending on the location of predrilling and landfall points. These ways are presented in Figure 4.6 [32].
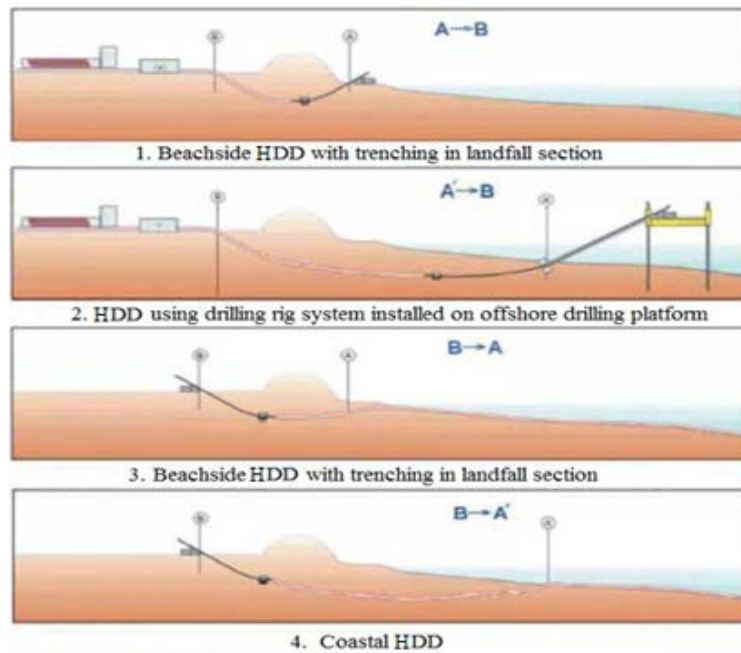
Figure 4.6. Methods of Horizontal Directional Drilling [32]

The construction of subsea pipeline onshore section by means of HDD method is preferable under the conditions of cliffed nature of the shore, strong current and significant wave impact which all totaled provide great complexities while pipeline trenching.

The intersection of the shoreline also can be carried out by the tunneling method. This method includes building up a tunnel from the shoreline to the offshore, assembling and pulling of the protective casing and pulling of pipe string. The tunnel is constructed by means of tunneling shield, driven by a jacking unit which is imbedded at a depth necessary for pipeline construction [32]. The microtunelling machine AVN1200T Herrenknecht is shown in Figure 4.7.

Figure 4.7. AVN1200T Herrenknecht Microtunelling Machine [32]

This method is seen as an alternative to HDD method. Tunneling technology allows specialists to construct pipelines in every class of soil: from unstable clay loam and water-bearing sand to hard rock. Also, this method has its extra advantages as it avoids the necessity for bottom dredging and gives less significant impact on the environment.

However, there are several examples of implementations of unique technological decisions of shore crossing design in the Arctic. One of those examples is the «Nortstar» project [5].

In this project the pipeline intersects the shoreline at the right angle. In order to make up for the warm expansion of the submerged pipeline sector there has been installed a corrugated pipe culvert around the vertical junction. The cliff of the shoreline is relatively low (0.6 m) The shoreline intersection takes place in secured shallow lagoon of Guider bay which is surrounded by two barrier islands named Stamp and Egg. This is the reason for the coastal erosion of the region to be shore crossing scheme is presented in Figure. 4.8.
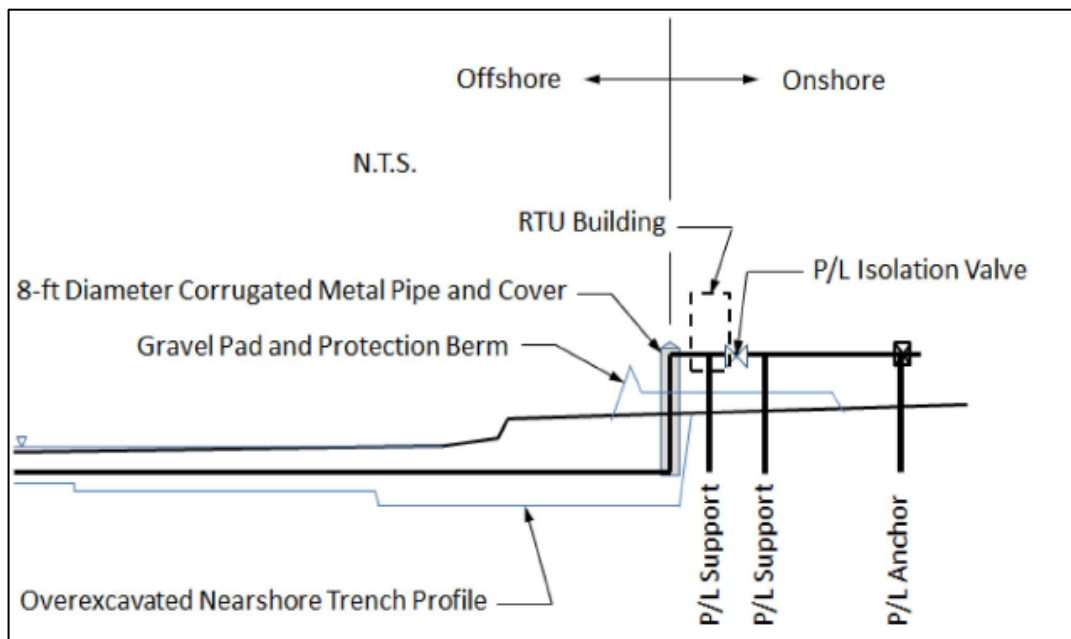
Figure 4.8. The «Nortstar» Project Shore Crossing Scheme [5]

Other elements of the landfall construction included gravel floor with a helicopter landing site, a remote telemetry unit for communication and power supplies, remote-controlled block valves, temperature and pressure sensors, and leakage check system. The permafrost soil was overexcavated across and replaced with solid soil in order to prevent permafrost thawing [5].

Thus, it can be summarized that while choosing a method for coastal intersection with underwater pipeline it is necessary to consider geotechnical setting of the sector, environmental conditions and

security standards as well. It is important to know that changing of in-situ conditions of Arctic shorelines can lead to accelerated growth of erosion processes.

4.7. Pipelaying Methods in the Arctic Region

Underwater pipeline laying in the Arctic region can be a complicating task due to harsh weather conditions, a short open water period and a lack of infrastructure. Also it should be considered that fragile Arctic environment must not be affected while performing all the necessary work.

Desighning pipeline laying in the Arctic area, it is vital to give a solution to several important questions. The first is equipment and vessel manufacturing, which would provide a possibility to work in harsh climate conditions. The second is elaborating safe methods of ice management. The third is improvement of ice and hydrometeorological forecasting systems and the last but not least is improving of logistics aspect that will allow mobilizing all necessary technical devices within a short period of time. All the above mentioned should be aligned with security conditions and natural environment protection.

Today there are two main variants of pipeline laying in the Arctic area [15]:

- Classical high-rate pipelaying techniques during summer open water season and with the adequate level of ice conditions control;
- Pipelaying techniques during winter season.

The key factor during the pipeline construction is the rate of pipelaying. Time should be managed in such a way so that pipelaying process is finished as soon as possible in order to make a full use of summer working season. Methods of horizontal pipelaying can provide the maximum speed of underwater pipeline construction. Such methods include S-lay, Flex-lay and Reel-lay methods [15].

The climate conditions in Arctic are harsh and severe so pipelaying vessels can be exposed to low temperature and, as a result, ice up. This can deal damage to both machinery and equipment. Therefore, there is a strong need in new class of vessels development. Such vessels would be able to carry out work in severe Arctic conditions. The characteristics of this new class must include improved shell plating, heated up helicopter platforms, emergency boat disposal domain, containers for fresh water heating, etc. In 2016 «Subsea 7» company built up a «Seven Arctic» vessel presented in Figure. 4.9. While pipelaying, this vessel uses Flex-lay technique, also it has strengthened body and helicopter platform completed with a heating system in order to prevent icing processes [43].

Figure 4.9. «Seven Arctic» Pipelaying Vessel [43]

«Heerema Marine Contractors» company that deals with underwater pipeline construction suggests the concept of ice-class reel ship «Mega Reel» (Figure. 4.10.). Such a vessel lays «pipe in pipe» pipelines with a diameter up to 460 mm with its deformation do not exceed 0.8%. Large diameter of the drum (61 m) makes it possible to achieve low level of plastic deformation. However, this method is not acceptable for concrete pipes. It is more preferable to use S-laying while working with concrete weight coated pipes of a large diameters [15].
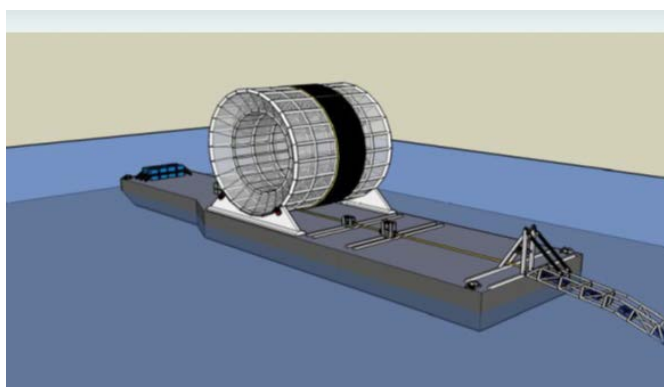
Figure 4.10. The Concept of Ice-class «Mega Reel» Reel Vessel [15]

«Hereema Marine Contractors» company is working out methods of sub-ice pipelaying. The development is focused on special machines which would be able to lay pipes under ice cover. A prime example of such a machine is a concept of immersible remote-controlled pipelayer for construction and installation work with a carrying capacity about 400 tons. The pipelayer is presented in Figure. 4.11.
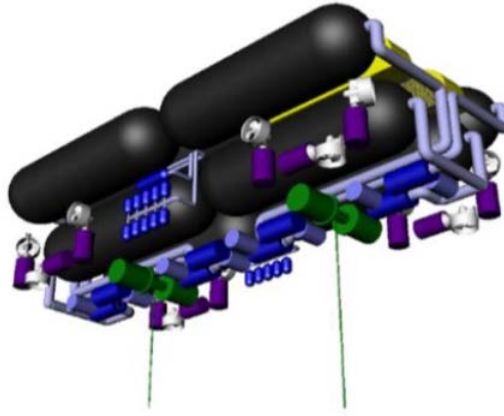
Figure 4.11. The Concept of Immersible Pipe Layer, «Hereema Marine Contractors» [15]

During freeze-up period in winter, it is possible to winch the pipeline through the bottom of the sea using sea ice as a prop for pipelaying equipment. The procedure sheet of this method is presented in Figure 4.12. This method was applied by American engineers during field development in Beaufort Sea.
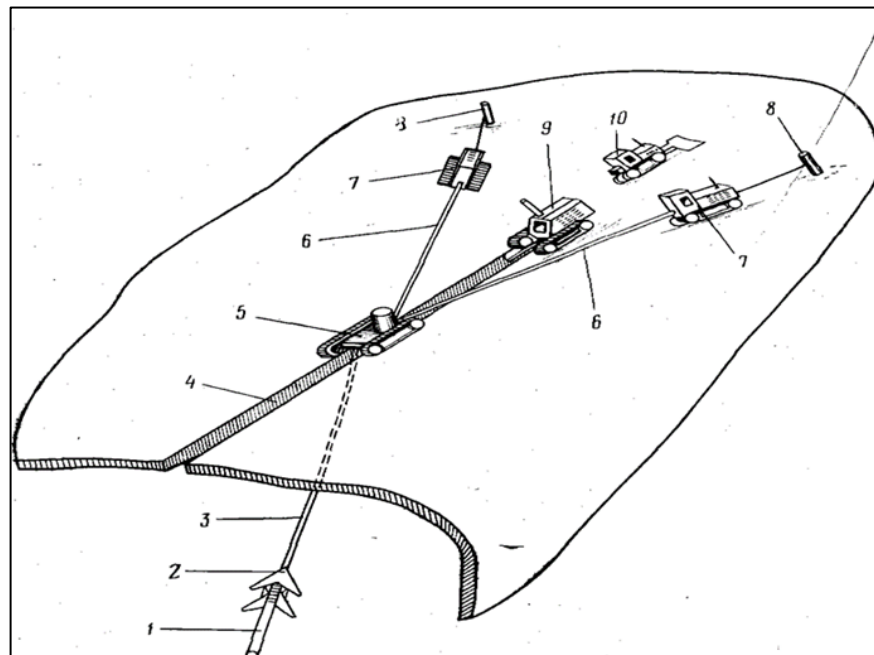
Figure 4.12. Scheme of Ice-base Pipeline Installation; 1 – pipeline; 2 – trenching plough; 3 – embedded cable rope; 4 – trench; 5 – traction carriage; 6 – cable ropes; 7 – winching tractors; 8 – pipe anchors; 9 – trench excavator; 10 – bulldozer padding fragmented ice [32]

Then multiple-cut trench excavator digs up a lane in the ice right in front of the carriage to pull a cable rope through the lane to the pipeline crown. Then a submerged mechanical plough digs up a trench to bury a pipeline into.

American scientists have made a research that has proved that the underwater pipeline installation by using shore ice as a prop for traction mechanisms is possible. It has been discovered that ice from 0.4 to 1m in thickness can stand heavy horizontal weighting, heavy enough to drag pipeline through the bottom [8].

As the implementation of this method had a great success in the Beaufort Sea, it may be stated that the method can be applied and for other Arctic regions where the ice cover is thick enough. However, this method considers the depth of pipelaying work. While working in deep water, the ice surface would be exposed to significant vertical weighting because of heaviness of the pipeline slack section and this can lead to ice cover destruction.

Thus, it can be summarized that the key factor during the pipeline construction in the Arctic is the rate of pipelaying. To date, S-lay method provides the highest speed of pipelaying (up to 500 MPH) and Reel-lay (up to 1000 MPH) [12]. Using these method while pipelaying, one should guarantee an adequate control over the ice situation. Also there is a necessity for modernization of vessels in order to work in severe climate conditions of the Arctic region. The American engineers' experience in Beaufort Sea has shown that it is possible to perform pipelaying works from ice on shallow depth, but there must be ice layer from 0.4 to 1 m in thickness. This method can potentially be applied while developing Tar Bay and the Gulf of Ob. Development of sub-rice pipelaying methods is also a promising area for specialists.

4.8. Pipeline Trenching Under the Arctic Conditions

The main problem in the development of offshore fields under the harsh Arctic conditions is the protection of underwater structures from ice gouging. The process pipeline trenching below maximum possible depth of ice keel scouring is the primary method to protect underwater pipelines.

The ice cover is one of the main problems of the construction of trenches in the Arctic. This may represent a number of logistical problems with an access to a vessel, the descent of equipment through the ice and power supply of equipment under water. In addition, extremes of temperatures can be a problem in terms of reliability and maintenance equipment.

The methods of trenching in the Arctic region can be conditionally subdivided into the ways, which are used during the summer (open water), and methods used during the winter. The methods used during the summertime include [11]:

 – The use of a plough
 – The use backhoe Dredge (BHD)
 – The use of the Cutter Suction Dredger (CSD)
 – The use of the Trailer Suction Hopper Dredge (TSHD)
 – Jetting
 – The use of mechanical trenchers.

The methods that are used during the winter (considering the ice cover):

 – The use of the plough
 – The use of backhoe dredges, installed on the ice

The main characteristics of each method are given in the Table 4.1.

Table 4.1. The main characteristics of trenching methods for Arctic pipelines [11]

Parameter	Plough	Jetting	Mechanical Trenching	TSHD	CSD	BHD
Max trench depth, m	2-3	3	4	>5	>5	>5
Max. trench width, m	8	3	2	>10	>10	>10
Max. bearing capacity of soil, KPa	400	100	40000	-	-	-
Max depth of trenching	1000	3000	1500	150	30	25
Max speed of trenching	200-1100	400	100-400	60	60	60
Possibility of excavation of boulders larger than 1 m	yes	no	yes	yes	yes	yes

The possibility of trenching before/after installation of a pipeline	Before \ after	Before \ after	Before \ after	before	before	before
A form of trench	"V"	Box/"V"	Box/"V"	Box/"V"	Box/"V"	Box/"V"
The possibility of use in the shore crossing	no	no	no	yes	yes	yes

The analysis of literary source revealed that nowadays there is no single technology for the trenching in Arctic. It is possible to use a combination of methods, such as using a plow to remove the top layer soft soil, then the use of a rock trencher for the excavation of hard soil and a jetting to clean out the trench before pipelaying.

Methods for pipeline trenching from the floating equipment should be carried out with high level of ice management.

During the trenching process in winter, it is necessary take into account the strength properties of the ice sheet; the ice can be artificially thickened.

The equipment should be modified in order to operate under the harsh environmental climatic conditions.

Usually the preference is given to the trenching methods before or during pipelaying to prevent damaging a left uncover pipeline by the processes of ice gouging.

The use of hydraulic dredgers can be limited due to the solid permafrost soil.

Thus, in this chapter, the main features of the design, construction and operation of subsea pipelines in the Arctic shelf conditions are considered.

In Russia, there is a project to develop the Shtokman gas condensate field (SGCF), located in the central part of the Barents Sea, 600 km from the coast, the sea depth reaches 346m. According to the explored reserves of natural gas, Shtokman is among the ten largest gas fields in the world; its reserves are estimated at 3.9 trillion m^3 of natural gas and about 56 million tons of gas condensate. This volume is comparable to global gas consumption over 1.3 years [40].

The importance of the Shtokman project is determined by several factors. The project will create the economic basis for the further development of the Russian Arctic shelf. Shtokman project will strengthen the energy security in the regional, European and global markets for the long term, supplying gas to meet growing energy demand.

In addition, the Shtokman project will create the basis for the transfer to Russia of modern management and production technologies for the development of offshore fields and, importantly, will ensure the utilization capacity of Russian industrial companies.

The project of the Shtokman field development envisages the building of an offshore trunk pipeline that will connect a floating production unit with onshore facilities. The length of the offshore section of the pipeline is 550 kilometers; the depth of the sea along the pipeline's route reaches 346 m [40].

In the design of offshore pipeline for the Shtokman field, the following factors should be taken into account: large sea depth, harsh climatic conditions, rugged bottom relief, the probability of gas hydrates formation, permafrost spreading in the bottom sediments.

Thus, the trunk pipeline for the Shtokman field is a unique project with regards to the construction of an offshore pipeline in Arctic conditions, and it is of interest not only for Russia, but also for the global practice of building offshore pipelines.

That is why the underwater pipeline for the Shtokman field was chosen as an illustrative example of the methods for determining the optimal pipeline design parameters, which in the future can be used in future projects for the construction of offshore underwater pipelines in the Russian Arctic shelf.

5. Subsea Pipeline Design for the Shtokman Gas Condensate Field

The trunk pipeline Shtokman gas condensate field was chosen as the design object. A brief characteristic of the project is given below.

5.1. General Information about the Field

The Shtokman gas condensate field was opened in 1988. It is situated in the Central part of the shelf of the Russian sector of Barents Sea, in the Northeast of Murmansk, at a distance of 600 km from the coast. The depth of the sea in this area ranges from 320 m to 350 m. Reserves of category C1 are 3.9 trillion cubic meters of gas and 56 million tons of gas condensate. The geographical position of the Shtokman field is shown in the Figure 5.1. [40]

Figure 5.1. Geographical Location of the Shtokman field [39]

5.2. Climatic and Meteorological Conditions of the Shtokman Field

The region of the Shtokman field is characterized by severe environmental conditions due to high waves, strong wind and currents, ice sheet and icebergs. The description of meteorological and climatic conditions is given below.

5.2.1. Water temperature

The maximum average monthly water temperature in the Shtokman field takes place in August, the minimum – in March and April. The absolute maximum temperature is 9 °C; the absolute minimum temperature is from 0 °C to -1 °C on the sea surface [22]. The apportionment of the average monthly sea water temperature through depth is presented in Table 5.1.

Table 5.1. The distribution of the average monthly temperature of sea water through depth [22]

Depth	Feb.	Mar.	April	May	Jan.	July	Aug.	Sep.	Oct.	Nov.	Dec.
0 m.	-0.5	-0.2	-0.81	-0.45	1.83	1.83	1.83	1.83	1.83	1.83	1.83
10 m.	-0.57	-0.2	-0.75	-0.46	0.87	0.87	0.87	0.87	0.87	0.87	0.87
20 m.	-0.56	-0.3	-0.75	-0.48	1.92	1.92	1.92	1.92	1.92	1.92	1.92
50 m.	-0.59	-0.56	-0.93	-0.52	0.68	0.68	0.68	0.68	0.68	0.68	0.68
100 m.	-0.63	-0.94	-0.94	-0.58	0.07				0.29	1.73	9.6
150 m.	-0.67	-0.97	-0.95	-0.77	-0.24				-0.48	0.8	0.5
200 m.	-0.76	-0.97	-0.95	-0.89	-0.3					0.25	0.4
250 m.	-0.92	-1	-0.97	0.93	-0.43				-0.95	-0.11	-0.78

5.2.2. Air temperature and relative humidity

The air temperature in the region of the Shtokman field varies from -9 °C in February to +15 °C in July. The absolute minimum is -38 °C. Negative temperatures last for 170-190 days a year [22]. Maximum air temperatures at the Shtokman field during the years are presented in the Table 5.2.

Table 5.2. The values of maximum air temperatures [22]

Month	Maximum air temperatures, °C		
	Return period, years		
	1	10	100
January	4	5	6
February	4	6	7
March	4	6	7
April	5	6	7
May	6	7	8
June	9	11	12
July	12	14	15
August	12	13	15
September	10	11	12
October	8	9	10
November	5	6	7
December	4	5	6
Year	12	14	15

The values of the minimum daily air temperature and relative humidity in the region of the Shtokman field are presented in table 5.3.

Table 5.3. The Values of minimum air temperature and relative humidity [22]

Month	Min. air temperature, °C					Relative humidity, %				
	Return period, years					Return period, years				
	1	5	10	50	100	1	5	10	50	100
Jan.	-11	-15	-18	-23	-26	89	85	82	77	74
Feb.	-13	-21	-24	-33	-36	87	79	76	67	64
Mar.	-15	-23	-27	-35	-38	85	77	73	65	62
Apr.	-12	-17	-19	-24	-25	88	83	81	76	75
May	-5	-9	-11	-16	-19	66	53	89	84	81
Jun.	0	-2	-2	-3	-3	80	75	74	71	70
Jul.	3	2	2	1	1	88	86	85	83	83
Aug.	4	3	2	2	1	92	88	87	85	84
Sep.	2	0	0	-1	-1	85	81	80	78	77
Oct.	-3	-6	-7	-8	-9	70	62	60	55	53
Nov.	-7	-10	-10	-12	-13	59	51	90	88	87
Dec.	-10	-13	-15	-17	-19	51	87	85	83	81
Year	-15	-23	-27	-35	-38	85	77	73	65	62

5.2.3. Winds, waves and currents

The table describing the mode of winds, currents and waves in the region of the Shtokman field is given below.

Table 5.4 Winds, currents and waves modes [22]

Parameter	Return period, years		
	100	10	1
Waves			
H_{max}, m	23.3	20.4	17.5
H_s, m	12.5	10.8	9
T_p ,s	17.2	16.1	15
Wind speed at the height of 10 m, m/s			
V1h	31	28	26
V10min	34	31	28
V1min	38	34	32
V3s	44	39	36
Current speed, cm/ s			
$U_{surface}$	88	76	64
U_{bottom}	39	36	32
The height of the wave crest, m	14.2	12.3	10.5

5.2.4. Ice conditions

The main distinctive feature of seasonal changes in the ice cover of the Barents Sea is that the sea never freezes completely, which is explained by the constant presence of warm Atlantic currents,

but at the same time the ice cover never melts completely. The greatest ice cover is usually observed in the second decade of April, the smallest - in late August and first half of September. In August — September, the anomalously warm years completely clear the sea of ice, and in the anomalously cold years the ice cover during these months remains at 40–50% of its area, mostly located in the northern regions. At the end of the most severe winters, over 90% of the sea's area is covered with powerful cohesive ice, and in especially warm winters, the greatest efficiency even in April does not exceed 55–60% [6]. The location of the ice edge in April in the area of the SGCF is shown in Figure 5.2.
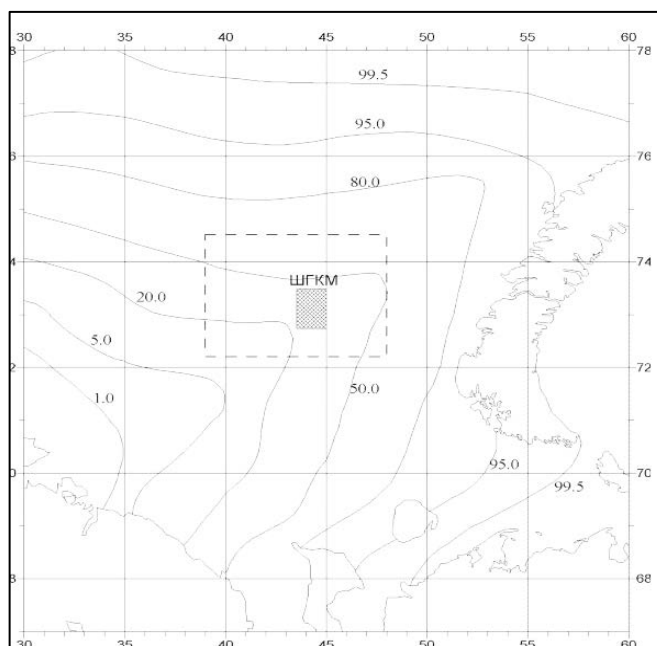
Figure 5.2. Probability of the Ice Edge Distribution in April in the area of the SGCF (%) [36]

The Barents Sea ice sheet consists of 58% of multiyear ice, 23% of massive ice (> 1 m) and 18% of new ice (less than 1 m thick). However, comprehensive information obtained as a result of a series of studies over the past decades shows that multi-year ice in the western part of the Barents Sea is quite rare. Thus, the most common type of ice in the Barents Sea is first-year ice of 1.9 m thick [17].

The glaciers of the Arctic archipelago (Spitsbergen, Franz Josef Land and Novaya Zemlya are potential sources of icebergs in the Barents Sea. It is impossible to exclude the possibility of the drift of icebergs from the Arctic basin, output glaciers of the Canadian Arctic Archipelago and the glaciers of Severnaya Zemlya, which can get into the Barents Sea through deep straits. On the closest to the Shtokman gas condensate field of the Novaya Zemlya archipelago of the sea coast of the Barents Sea there are 19 outflow glaciers of the northern island of Novaya Zemlya, of which

10 are I have the largest outlet glaciers of the Eurasian Arctic islands. The length of the front of ice is 117 km [36].

Figure 5.3 presents the results of a visual study of the location of icebergs and ice edges in the SGCF region for the period from May 1-15, 2003 [36].
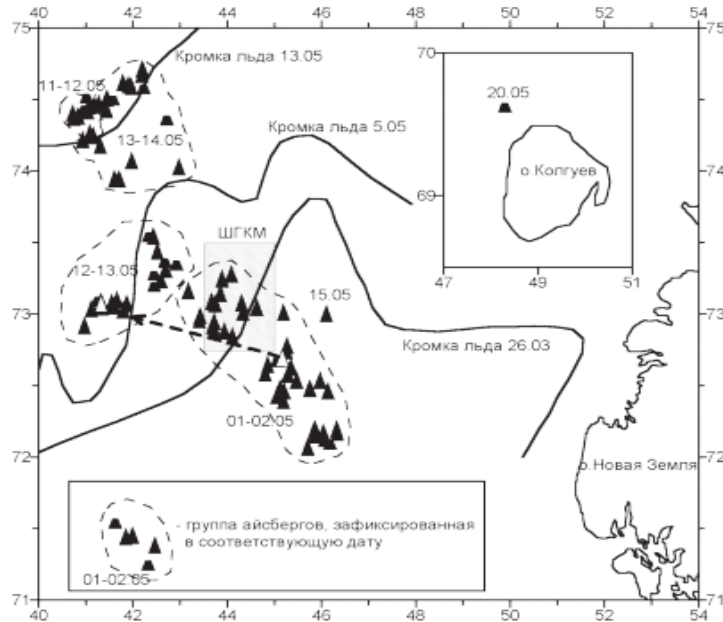
Figure 5.3. Location of Icebergs in the SCGF Area for the Period from May 1-15, 2003 [36]

The maximum recorded horizontal dimensions of the iceberg were 190x430 m, and the maximum measured height was 20.8 m. The largest mass was 3.7 million tons, and the average mass of icebergs was 870 thousand tons, the underwater part reached 90 m [36].

According to the results of the expedition of 2003, it can be said that there is a real iceberg danger for the designed floating production unit and its communications for the shipment of products, which requires increased level of the ice management in the region. It is necessary to improve the methods of tracking ice drift, as well as methods of active protection against icebergs.

Protection of underwater structures and communications is required to a lesser extent, due to the significant depths of the SGCF region.

5.3 Basic Technological Solutions

The development of the Shtokman gas condensate field will be organized with the help of subsea production units, the extracted products from which will be transported along flexible production risers to the floating production unit, here the gas will be pretreated. The recycled gas is supplied

via flexible export risers to the underwater pipeline manifold, which connects the risers to a twin trunk pipeline, through which products will be transported to onshore facilities to the village of Teriberka of Murmansk region [40]. The scheme of the SGCF development is shown in Figure 5.4.
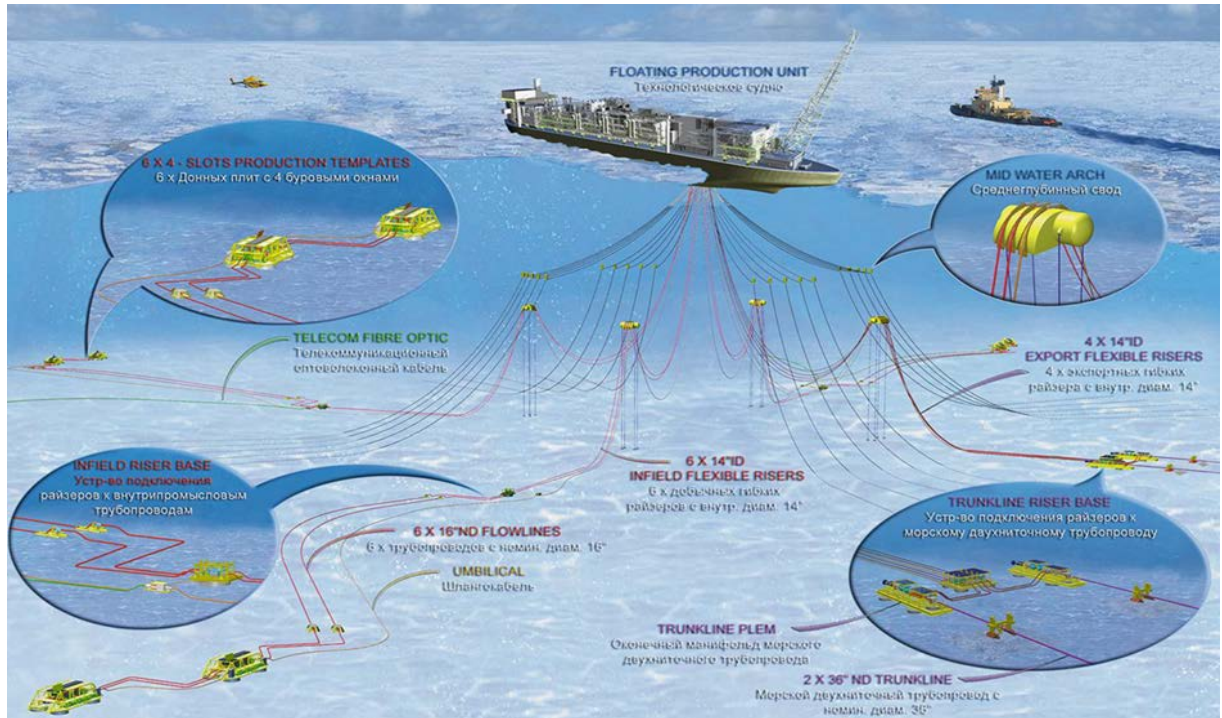
Figure 5.4 The Scheme of Shtokman Field Development [24]

Gas, together with the gas condensate comes from the subsea production units through two pipelines. The pipeline access points will be located on the north shore of the Kola Peninsula in Opasov Bay.

The coastal part of the offshore pipeline from its access to the shore to the slugcatcher at the gas treatment complex will be laid under the ground and have a length of 10 km. After the slugcatcher, the flow will be divided into two parts: half of the gas will go to the gas treatment unit, and the other to the liquefied natural gas plant for further processing and liquefaction. The processed gas from the gas treatment unit will be supplied to the Murmansk-Volokhov trunk pipeline, which is part of the unified gas pipeline system of «Gazprom» company. The recovered condensate will be stabilized and sent to storage and subsequent shipment to Korabelnaya Bay [40].

5.4. Pipeline Routing

When choosing the optimal route of the underwater pipeline for SGCF, the options for leaving the Barents Sea to land in the settlements of Pechenga and Teriberka were considered, and the option of passing the pipeline through the White Sea was also considered.

Analysis of technical and economic indicators of possible options for gas pipeline routes that provide gas transportation from SGCF to the unified gas supply system (UGSS) of Russia revealed the advantage of the SGCF-Teriberka-Volkhov direction. The advantage of this route option: is the minimum distance from the field to the point of connection to the Unified Gas Supply System; the shortest option for the gas pipeline route to areas with developed industrial and social infrastructure (roads, railways, airports, towns and cities, construction materials careers) [26].

Within the offshore section along the bottom of the Barents Sea, the offshore section of pipeline will pass through the Central Hollow, the slopes of the Murmansk Bank, then along the bottom of the Opasov Bay before reaching the shore [24]. The route of the SGCF -Teriberka trunk pipeline is shown in Figure 5.5.

Figure 5.5. The Route of Shtokman Trunk Pipeline [24]

The main pipeline route features [24]:

Length:

- – Underwater section: 550 km;
- – Onshore section: 8km;

Route Characterisation:

- – Pockmarks- elongated features-150m × 100m × 5m deep;
- – Unhazardous area- 34%;

Water depth:

- – Maximum- 350m;
- – Mostly- approximately 250m;

Seabed:

- – Generally soft or very soft clays
- – Rock in shore approach

Based on the bathymetry of the Barents Sea along the pipeline route, a potential bottom profile was suggested (Figure 5.6).
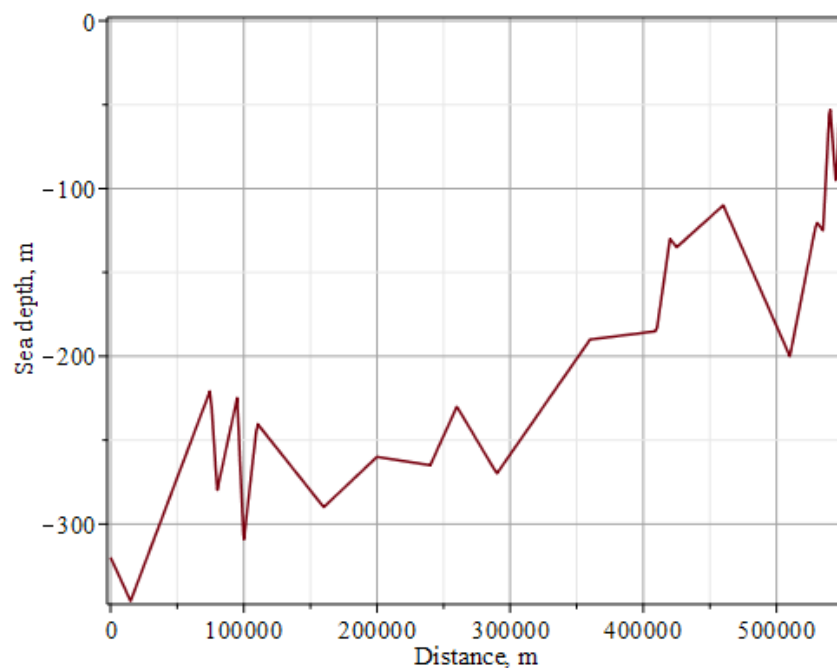

Figure 5.6. Bottom Profile along Pipeline route

5.5 Calculation of the Pipeline Wall Thickness

The choice of pipeline wall thickness is one of the key design issues based on methods for calculating the strength and stability of any structure, ultimately ensuring the safety of the offshore gas pipeline operation.

According to the project of «Shtokman Development AG» («SDAG»), each of the two pipelines will be assembled from pipes with the steel grade X70, with a constant diameter of 34 inches (863.6 mm); the capacity of each line is 38 million m^3/day of gas [24].

The calculation of the wall thickness was made in accordance with the Norwegian DNV-OS-F101 Standard «Underwater Pipeline Systems», this standard was approved by Gazprom in 2006 (STO Gazprom 2-3.7-050-2006).

In this paper, the calculation of wall thickness is made taking into account the following possible failures, formulated in the concept of limiting states:

- − Bursting limit state;
- − Local buckling limit state (collapse);
- − Global buckling limit state.

Before the calculation part, it is necessary to define some terms:

Bursting is a type of failure when a pipe ruptures due to high internal pressure.

Local buckling (collapse) is a type of failure implies a significant deformation of the cross section, due to the external pressure impact.

Global buckling is a type of failure implies local buckle that propagates through the length of the pipe, due to the external pressure impact [2].

Serviceability Limit State (SLS): A condition which, if exceeded, renders the pipeline unsuitable for normal operations.

Ultimate Limit State (ULS): A condition which, if exceeded, compromises the integrity of the pipeline.

Fatigue Limit State (FLS): An ULS condition accounting for accumulated cyclic load effects.

Accidental Limit State (ALS): An ULS due to accidental (in-frequent) loads [2].

Input data for calculating the wall thickness of the pipeline are presented in Table 5.5.

Table 5.5. Input data for pipeline wall thickness calculation [24]

Parameter	Designation	Value	Unit
Pipeline Dimensions			
Nominal internal diameter	D	863.6	mm
Design flow rate	Q	38 mln	m^3/day
Corrosion tolerance	t_{corr}	1.5	mm
Fabrication thickness tolerance	t_{fab}	1	mm
Lifetime	-	50	year
Ovalization	f_0	1.5	%
Safety class	-	Normal	
Steel Characteristics			
Steel grade	X70		
Steel density	ρ	7850	kg/m^3
Young's modulus	E	210	GPa
Poisson's ratio	υ	0.3	-
Standart minimum yield strength	SMYS	482.7	MPa
Specified minimum tensile strength	SMTS	565.4	MPa
Anisotropy coefficient	α_A	1	
Material Strength factor	α_U	0.96	
Fabrication factor	α_{fab}	0.93	
De-rating of SMYS (75 ^{o}C)	$f_{y,temp}$	14	MPa
De-rating of SMTS (75 ^{o}C)	$f_{u,temp}$	14	MPa
Product Information			
Pumped product	Gas with some condensate		
Product density	ρ_i	0.87	kg/m^3
Design internal pressure	p_d	18.9	MPa
Incidental to design pressure ratio	γ_{inc}	1.1	
Maximum inlet temperature	T_{max}	75	℃
Environmental characteristics			
Ambient temperature	T_e	-1.8	℃
Max sea depth	h_l	346	m

5.5.1. Pressure containment (bursting)

Pressure containment resistance shall be calculated based on wall thickness as follows: [2]:

$$t_1 = t - t_{fab} - t_{corr} \qquad (5.1)$$

where t – nominal wall thickness, mm; t_{fab} – fabrication thickness tolerance, mm; t_{corr} – corrosion tolerance, mm.

The pressure containment shall fulfil the following criteria: [2]:

$$p_{ii} - p_e \leq \frac{p_b(t_1)}{\gamma_{sc} \cdot \gamma_m} \qquad (5.2)$$

where p_{li} – local incidental pressure, Pa; p_e – external pressure, Pa; $p_b(t)$ – pressure containment resistance, Pa; γ_{sc} –safety class resistance factor; γ_m – material resistance factor.

External pressure is defined as [2]:

$$p_e = \rho \cdot g \cdot h_l \qquad (5.3)$$

where ρ – seawater density, kg/m^3; g – acceleration of gravity, m/s^2; h_l – sea depth, m.

Local incidental pressure is calculated as [2]:

$$p_{li} = p_d \cdot \gamma_{inc} \qquad (5.4)$$

where p_d – design pressuree, Pa; γ_{inc} – incidental to design pressure ratio;

The incidental to design pressure ratio γ_{inc} is usually assumed to be 1.1. The values of the safety class resistance factor γ_{sc} depend on the safety class and are given in the Table 5.6. The safety class resistance factor γ_{sc} is taken equal to 1.138, corresponding to the normal safety class. The material resistance factor γ_m depends on the type of the limit state and is determined according to Table 5.7. The material resistance factor γ_m is taken equal to 1.15, corresponding to the Ultimate Limit State (ULS).

Table 5.6. Safety class resistance factor, γ_{sc} [2]

	γ_{sc}		
Safety class	Low	Medium	High
Pressure containment	1.046	1.138	1.308
Other	1.04	1.14	1.26

Table 5.7. The material resistance factor, γ_m [2]

Limit state category	SLS/ULS/ALS	FLS
γ_m	1.15	1.0

The pressure containment resistance $p_b(x)$ is defined as [2]:

$$p_b(x) = Min\left[p_{b,s}(x); p_{b,u}(x) \right] \qquad (5.5)$$

Yielding limit state [2]:

$$p_{b,s}(x) = \frac{2 \cdot x}{D - x} \cdot f_y \cdot \frac{2}{\sqrt{3}} \qquad (5.6)$$

where D – internal diameter of pipe, mm; f_y – yield stress design value, Pa; f_u – tensile strength design value, Pa.

Bursting limit state [2]:

$$p_{b,u}(x) = \frac{2 \cdot x}{D - x} \cdot \frac{f_u}{1.15} \cdot \frac{2}{\sqrt{3}}$$

(5.7)

In the above formulas, x shall be replaced by t_1 or t_2 as appropriate.

Yield stress design value f_y and tensile strength design value f_u are defined as following [2]:

$$f_y = (SMYS - f_{y,temp}) \cdot \alpha_U$$

(5.8)

$$f_u = (SMTS - f_{u,temp}) \cdot \alpha_U \cdot \alpha_A$$

(5.9)

where $f_{y,temp}$ – derating value due to the temperature of the yield stress, Pa; $f_{u,temp}$ – derating value due to the temperature of tensile strength, Pa; SMYS -standart minimum yield strength, Pa; SMTS – specified minimum tensile strength, Pa; α_A – anisotropy factor; α_U - material strength factor.

Anisotropy factor $\alpha_A = 0.95$ for axial direction, $\alpha_A = 1$ for other cases; material strength factor α_U is determined by Table 5.8.

Table 5.8. Material strength factor, α_U [2]

Factor	Normally	Supplementary requirement U
α_U	0.96	1.0

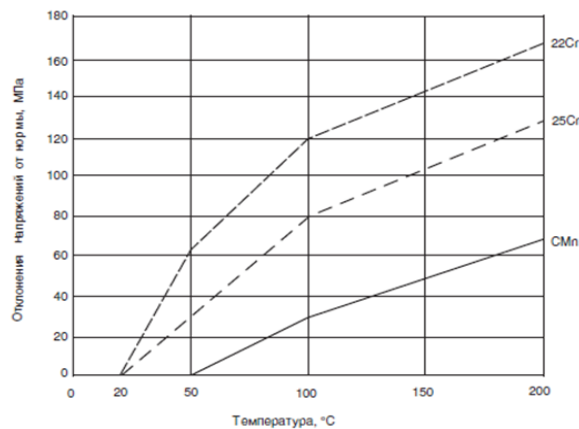The parameters $f_{u,temp}$ and $f_{y,temp}$ can be determined according to Figure 5.7

Figure 5.7. Proposed De-rating Values for Yield Stress of C-Mn and Duplex Stainless Steels (DSS). [2]

Figure 5.8 shows the results of calculations of the minimum wall thickness of the pipeline along its length according pressure containment criteria. Obviously, the pipeline must provide the maximum pressure containment resistance of the internal pressure on the surface, where the external pressure is equal to zero; here the minimum wall thickness is equal to 25.1 mm.
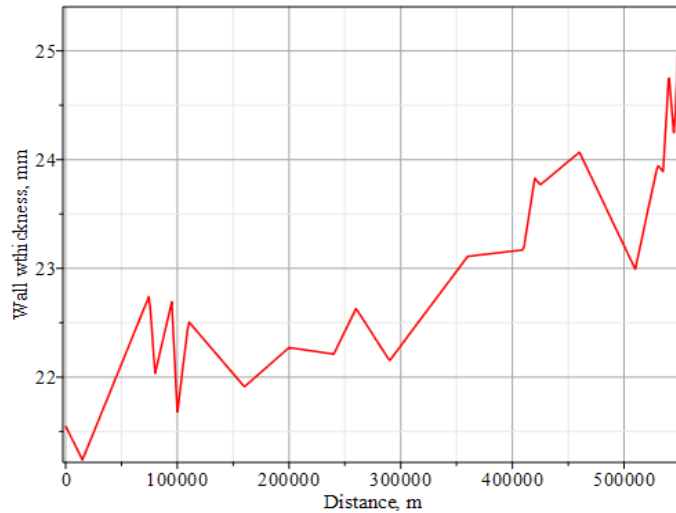
Figure 5.8. Change in the Minimum Wall Thickness along the Pipeline according Pressure Containment Criteria

5.5.2 Local buckling (collapse)

The external pressure at any point along the pipeline shall meet the following criterion (system collapse check) [2]:

$$p_e \leq \frac{p_c}{1.1 \cdot \gamma_m \cdot \gamma_{sc}}$$ (5.10)

where p_c – characteristic collapse pressure, Pa;

The characteristic resistance for external pressure p_c (collapse) shall be calculated as: [2]:

$$(p_c - p_{el}) \cdot (p_c^2 - p_p^2) = p_c \cdot p_{el} \cdot p_p \cdot f_o \cdot \frac{D}{t_2}$$ (5.11)

where p_{el} – elastic collapse pressure, Pa; p_p – plastic collapse pressure, Pa; f_o – ovalisation, %.

Elastic collapse pressure p_{el} is calculated as [2]:

$$p_{el} = \frac{2 \cdot E}{1 - v^2} \cdot \left(\frac{t_2}{D}\right)^3$$ (5.12)

63

where E – Young's module, Pa; v – Poison's ratio.

Plastic collapse pressure p_p is equal to [2]:

$$p_p = 2 \cdot f_y \cdot \alpha_{fab} \cdot \left(\frac{t_2}{D}\right)$$

(5.13)

where α_{fab} – fabrication factor, which is determined by Table 5.9.

Table 5.9. Fabrication factor, α_U [2]

Pipe	Seamless	UO & TRB & ERW	UOE
α_{fab}	1	0.93	0.85

Figure 5.9 shows the change in the minimum wall thickness along the pipeline according to the local buckling criteria. The pipeline section is most susceptible to collapse at a maximum depth of 346 m; here the minimum wall thickness must be equal at least 20.6 mm.

Figure 5.9. Change in the Minimum Wall Thickness along the Pipeline according Local Buckling Criteria

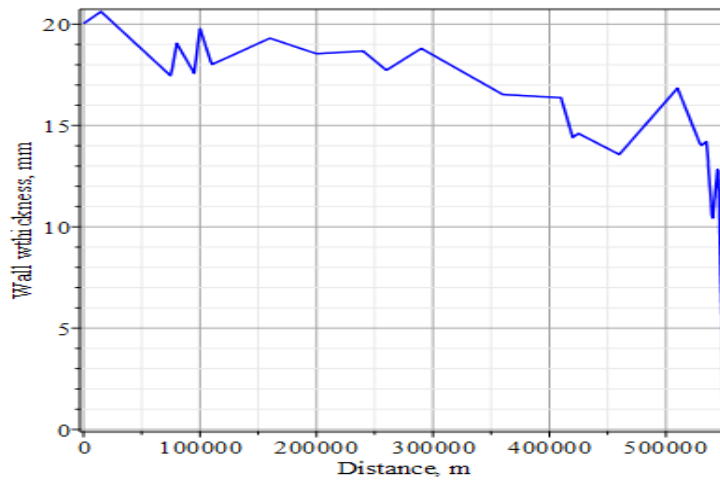Figure 5.10 shows the changes in the minimum wall thickness along the pipeline according to pressure containment and local buckling criteria.

Figure 5.10. Change in the Minimum Wall Thickness along the Pipeline according Local Buckling and Pressure Containment Criteria

From Figure 5.9 it can be seen that the defining criterion for the minimum wall thickness selection is the pressure containment resistance (bursting).

Thus, we take the wall thickness equal to 25.1mm. After the nominal wall thickness is chosen, it is necessary to check the pipe for the criterion of propagating buckling.

5.5.3. Propagating buckling

Propagation buckling cannot be initiated unless local buckling has occurred. In case the external pressure exceeds the criteria given below, buckle arrestors should be installed and spacing determined based on cost and spare pipe philosophy. The propagating buckle criterion reads [2]:

$$p_{pr} = 35 \cdot f_y \cdot \alpha_{fab} \cdot \left(\frac{t_2}{D}\right)^{2.5} \tag{5.14}$$

External pressure at any point along the pipeline shall meet the following criteria (propagating buckling check) [2]:

$$p_e \leq \frac{p_{pr}}{\gamma_m \cdot \gamma_{sc}} \tag{5.15}$$

where p_{pr} – propagating buckling pressure, Pa.

Figure 5.11 shows the change in the minimum wall thickness along pipeline according to propagating buckling criteria.
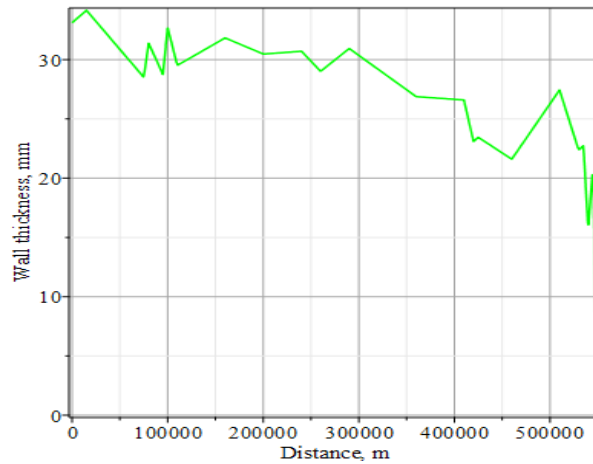
Figure 5.11. Change in the Minimum Wall Thickness along the Pipeline according Propagating Buckling Criteria

Just as in the case of local buckling, the pipeline section that is most susceptible to propagating buckling is located at maximum depth of 346m. The minimum wall thickness according to the propagating buckling criterion is 34.6 mm. However, it is not economically feasible to use pipes with such wall thickness. Moreover, there may be difficulties associated with the installation of the pipeline, due to the large weight of pipes, also there will be large loads on the stinger of pipelaying vessel, as well as the need to create large tension forces, in order to maintain pipeline integrity. Usually buckle arrestors shall be installed on the sections of pipeline where the phenomenon of propagating buckling is possible.

Changes in the minimum wall thickness along the pipeline according propagating buckling and pressure containment criteria are presented in the Figure 5.12.
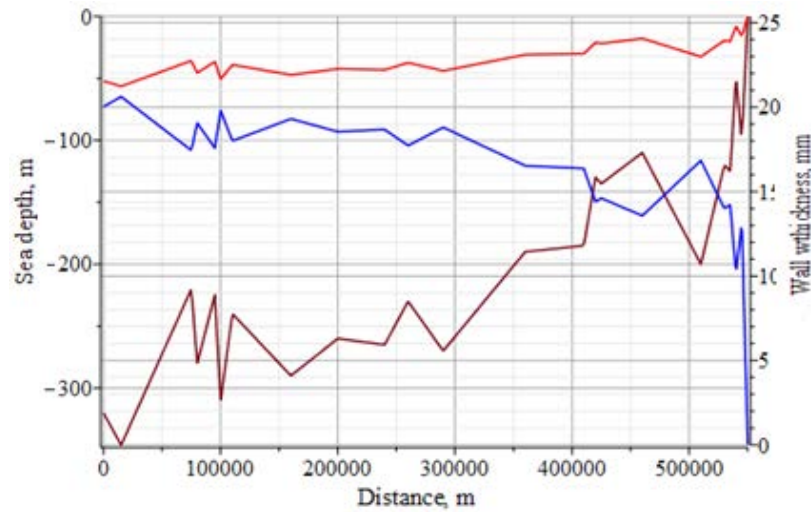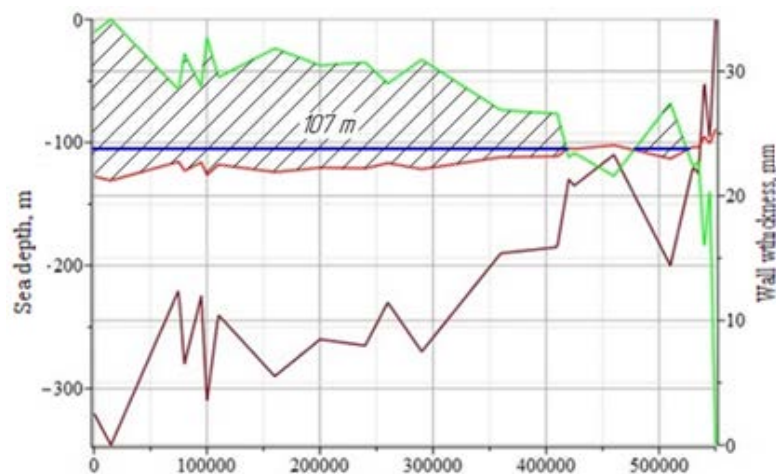

Figure 5.12. Changes in the Minimum Wall Thickness along the Pipeline according Propagating Buckling and Pressure Containment Criteria

66

From Figure 5.12 it follows that the installation of buckle arrestors is necessary on pipeline sections located at the depths greater than 107 meters.

Thus, the nominal wall thickness for the trunk gas pipeline for the Shtokman field is 25.1 mm, installation of buckle arrestors is required in the sections of the pipeline located at a depth of more than 107 meters

5.6. On-Bottom Stability Analysis

An important task in the design of the pipeline is to ensure its stable position at the bottom. Underwater pipeline during operation is affected by hydrodynamic loads from waves and currents, which can lead to displacement of pipeline. Usually pipelines are weighted by concrete coatings. In this section the minimum wall thickness of concrete coating for Shtokman pipeline are determined.

On-bottom stability analysis is made in accordance with the Norwegian standard DNV-RP-E305 (1988). According to this standard, there are three methods for analyzing the lateral stability of a pipeline at the bottom:

- – Dynamic lateral stability method;
- – Generalized lateral stability method;
- – Absolute lateral stability method.

In this work, the absolute lateral stability method is used, which is based on the equation of static balance of forces acting on a submerged pipeline (Figure 5.13).

Figure 5.13. Forces Acting on a Submerged Pipeline [24]

Table 5.10. Input data for on-bottom stability analysis [2, 22, 24]
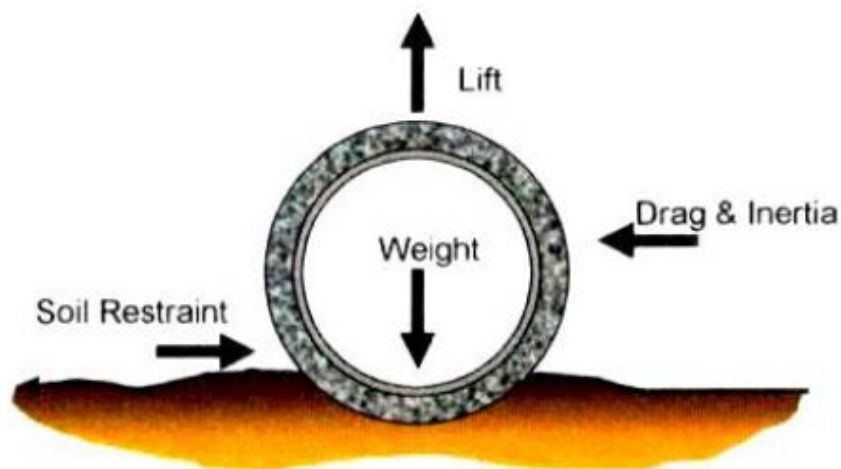
Parameter	Designation	Value	Unit
Pipeline Data			
Internal diameter	D	863.6	mm
Pipeline wall thickness	t	25.1	mm
Steel density	ρ_s	7850	kg/m^3
External corrosion coating thickness	t_{cc}	3	mm
External corrosion coating density	ρ_{cc}	1400	kg/m^3
Product density	ρ_i	0.87	kg/m^3
Seawater density	ρ_w	1025	kg/m^3
Concrete coating density	ρ_c	3040	kg/m^3
Coefficient of concrete water absorption	a	3	%
Environmental Data			
Significant 1year wave height	H_{1s}	9	m
Significant 100 year wave height	H_{100s}	10.8	m
Spectral peak period of 1year wave height	T_{1p}	15	s
Spectral peak period of 100 year wave height	T_{100p}	16.1	s
Extreme current velocity at 1 m above the seabed	U_r	0.32	m/s
Angle of attack – wave	α_w	90	deg
Angle of attack – current	α_c	90	deg
Height of measured current	Z_r	1	m
Kinematic viscosity of seawater	υ	1.13*10^{-6}	m^2/s
Soil data			
Soil type		clay	
Roughness of clay	z_o	0.005	mm
Coefficient of soil friction	μ	0.7	

First, it is necessary to find wave parameter, Tn [3]:

$$T_n = \sqrt{\frac{h_l}{g}} \tag{5.16}$$

Then we should determine the ratio of Tn to Tp. (λ):

$$\frac{T_n}{T_p} = \lambda \tag{5.17}$$

where T_p – spectral peak period of wave, s.

To calculate significant water velocity U_s, it is necessary to define parameter $\dfrac{U_s \cdot T_n}{H_s}$, which is calculated as following: [3]:

$$\frac{U_s \cdot T_n}{H_s} = (80.052\lambda^5 - 141.85\lambda^4 + 90.988\lambda^3 - 22.782\lambda^2 + 0.3772\lambda + 0.4967) \tag{5.18}$$

where H_s – significant wave height, m.

After the parameter $\dfrac{U_s \cdot T_n}{H_s}$ is determined, we can calculate significant water velocity U_s.

Next, it is necessary to calculate zero-up crossing period T_u. To do this, we should determine the ratio T_u/T_p [3]:

$$\frac{T_u}{T_p} = (14.491\lambda^4 - 16.788\lambda^3 + 5.5237\lambda^2 + 1.0172\lambda + 0.7116) \qquad (5.19)$$

After the value of T_u/T_p is determined, we can calculate zero-up crossing period Tu.

The next step is calculation of the current velocity perpendicular to the pipeline [3]:

$$U_c = U_r \cdot \left(\frac{\cos \alpha_c}{\ln\left(\dfrac{Z_r}{z_o}+1\right)} \right) \cdot \left(\left(1+\frac{z_o}{D_o}\right) \cdot \ln\left(\frac{D_o}{z_o}+1\right) - 1 \right) \qquad (5.20)$$

where D_o – overall pepe diameter, mm; Z_r – height of measured current above bottom, m; z_o – roughness of clay, mm.

Now it is necessary to define overall pepe diameter D_o [3]:

$$D_o = D + 2t + 2t_c + 2t_{cc} \qquad (5.21)$$

where t_c – concrete coating thickness, mm; t_{cc} – corrosion coating thickness, mm.

Further, it is necessary to determine the weight per unit length of the submerged pipeline, taking into account the concrete, corrosion coatings, as well as the weight of pumped product.

Weight per unit length of steel pipe:

$$W_s = \pi \cdot (D-t) \cdot t \cdot \rho_s \qquad (5.22)$$

where ρ_s – steel density, kg/m^3.

Weight per unit length of corrosion coating:

$$W_{cc} = \pi \cdot (D+t_{cc}) \cdot t_{cc} \cdot \rho_{cc} \qquad (5.23)$$

where ρ_{cc} – corrosion coating density, kg/m^3.

Weight per unit length of concrete coating:

$$W_s = \pi \cdot (D + 2 \cdot t_{cc} + t_c) \cdot t_c \cdot \rho_c \cdot a \qquad (5.24)$$

where ρ_c – concrete coating density, kg/m³; a – coefficient of concrete water absorption, %.

Weight per unit length of pumped product:

$$W_i = \pi \cdot \frac{(D - 2 \cdot t)}{4} \rho_i \qquad (5.25)$$

where ρ_i – product density, kg/m³

Weight per unit length of pipeline in air:

$$W_{air} = (W_s + W_{cc} + W_i) \cdot g \qquad (5.26)$$

Buoyancy force per unit length:

$$B = \frac{\pi \cdot D_o^2}{4} \cdot \rho_w \cdot g \qquad (5.27)$$

Therefore, the weight per unit length of the submerged pipeline is determined as follows [3]:

$$W_{sub} = W_{air} - B \qquad (5.28)$$

Next, we should determine the ratio U_c/U_s [3]:

$$M = \frac{U_c}{U_s} \qquad (5.29)$$

Keulegan number is calculated as following [3]:

$$K = \frac{U_s \cdot T_u}{D} \qquad (5.30)$$

The stability criteria for Simplified Static Stability Analysis is following [3]:

$$\left(\frac{W_{sub}}{F_W} - F_L \right) \cdot \mu \geq F_D + F_I \qquad (5.31)$$

where F_D – drag force per unit, N/m; F_L – lift force per unit, N/m; F_I – inertia force per unit length, N/m; F_W – calibration factor; μ – soil friction coefficient.

The forces are calculated by the following formulas [3]:

$$F_D = \frac{1}{2} \cdot \rho \cdot C_D \cdot D \cdot (U_s \cos\theta + U_c) |U_s \cos\theta + U_c| \qquad (5.32)$$

$$F_L = \frac{1}{2} \cdot \rho \cdot C_L \cdot D \cdot (U_s \cos\theta + U_c)^2 \qquad (5.33)$$

$$F_I = \frac{1}{4} \cdot \pi \cdot \rho \cdot C_M \cdot D^2 \cdot a_w \cdot \sin \theta \qquad (5.34)$$

where θ – wave phase angle, deg; a_w – particle acceleration normal to pipe axis m/s^2; C_D – drag coefficient; C_L – lift coefficient; C_I – inertia coefficient.

Water particle acceleration normal to pipe axis is calculated as follows [3]:

$$a_w = \frac{2 \cdot \pi \cdot U_s}{T_u} \qquad (5.35)$$

Calibration factor F_w, is determined as follows [3]:

- $F_w = 1.0$ if $K \leq 5.5$;
- $F_w = 1.2$ if $M \geq 0.8$;
- $F_w = [1.3 - (M - 0.7)]$ if $0.6 < M < 0.8$;
- $F_w = 1.4$ if $0.4 \leq M \leq 0.6$;
- $F_w = [1.5 - (M - 0.3)]$ if $0.2 < M < 0.4$;
- $F_w = 1.6$ if $M \leq 0.2$.

The drag coefficient C_D, lift coefficient C_L and inertia coefficient C_I have the following values [3]:

- $C_D = 0.7$, if $Re > 3*10^5$ or $M < 0.8$, in other cases $C_D = 1.2$;
- $C_L = 0.9$;
- $C_M = 3.29$.

The Reynolds number is determined by the formula [3]:

$$Re = \frac{(U_c + U_s)}{\nu} \qquad (5.36)$$

where ν – kinematic viscosity of seawater, m^2/s.

Converting the expression (5.31), we obtain the following expression to determine the minimum weight of the pipe:

$$W_{sub} \geq \left(\frac{F_D + F_I + F_L \cdot \mu}{\mu} \right) \cdot F_W \qquad (5.37)$$

Figure 5.14 presents the results of calculations of the minimum thickness of the concrete coating along the pipeline.
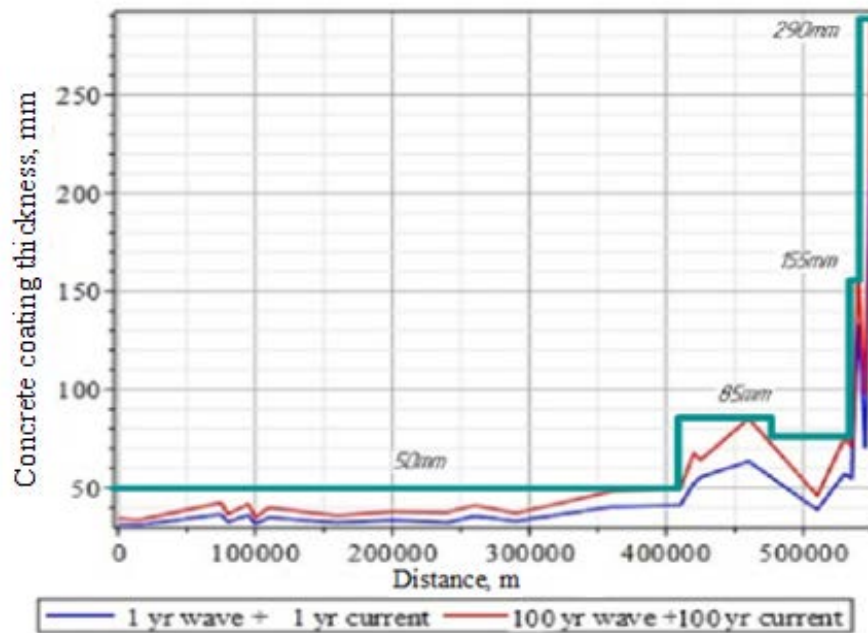
Figure 5.14. Change in the Minimum Concrete Coating Thickness along the pipeline

Calculations were made taking into account the hydrodynamic loads of 1 year and 100 year waves and currents. In accordance with the project of «SDAG», the design life of the pipeline is 50 years, therefore it is necessary to take into account the hydrodynamic loads of waves and currents with a 100 year return period [24].

The pipeline was conditionally divided into several sections, with different values of the thickness of the weighting coating. From figure 5.14 it can be seen that for a stable position of the greater part of the pipeline (the first 407 km), concrete coating of 50 mm thickness (with a density of 3040 kg/m^3) is required.

At the landfall areas, there is a sharp increase in the required thickness of the concrete coating; this can be explained by high influence of the hydrodynamic effects of waves and currents in shallow waters. Typically, the maximum thickness of the concrete coating for underwater pipelines is 150 mm. In order to avoid the displacement of the pipeline in the coastal zone, the pipeline must be covered with a 150 mm concrete coating, additionally, it must be trenched. According to the project of «SDAG», the last kilometer of the trunk pipeline will be trenched at depth of 1.6 to 2.1 meters [24].

5.7 Analysis of Pipeline Stress-Strain State during Installation

The most suitable method of installation of trunk pipeline for SGCF is S-lay. This technology allows to lay concrete offshore pipelines with a diameter of up to 60 inches (1524 mm) at depths of up to 500m [12].

There two critical sections of the pipeline during its installation by S-lay – overbend and sagbend, presented in the Figure 5.15. In these sections, there are stresses in the pipeline caused by affect of tension force from tensioners, bending moments, as well as external pressure. This can lead to the occurrence of local buckling (collapse) of the pipeline, which can further lead to a global buckling (Figure 5.16) [14].
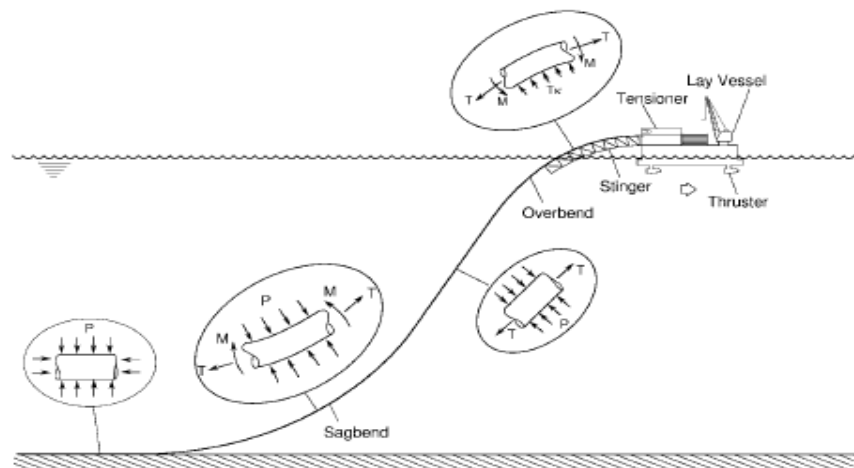
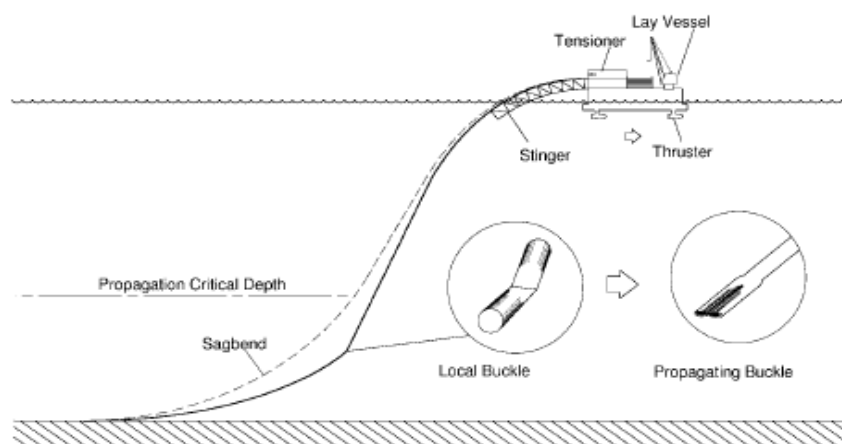Figure 5.15. Scheme of S-lay Pipeline Installation and Associated Pipeline Loadings. [14]

Figure 5.16. Scheme of the Initiation of a Propagating Buckle in a Pipeline from a Local Bending Buckle during S-lay Installation. [14]

To avoid the integrity damage of the pipeline, during installation, it is necessary to analyze the stress-strain of pipeline during its installation, and determine the following parameters:

- − Tension force at vessel;
- − Horizontal lay tension;
- − Maximum strain on stinger;
- − Maximum curvature in sagbend;
- − Maximum moment in sagbend;
- − Horizontal distance from vessel to touch-down;
- − Pipe length in free span;
- − Minimum horizontal lay radius.

Calculations were made for a section of a concrete pipeline with a 50 mm concrete coating thickness (section 5.5), laid at maximum depth (346 m). The initial data for stress-strain analysis is presented in table 5.11.

Table 5.11. Input data for stress-strain analysis

Parameter	Designation	Value	Unit
Overall Diameter	D_o	1020	mm
Wight of sobmerged	W_{sub}	1865	N/m
Stinger radius	R_s	100	m
Departure angle	α_{lay}	45	deg
Slight inclination	α_s	0	deg
Height above water	h	10	m
Girth weld factor	α_{gw}	0.88	
Strain resistance	$\gamma\xi$	2.5	
Coefficient of soil friction	μ	0.7	
Water depth	h_l	346	m

During S-Lay, the pipeline's shape is approximated as a catenary as shown in Figure 5.17.
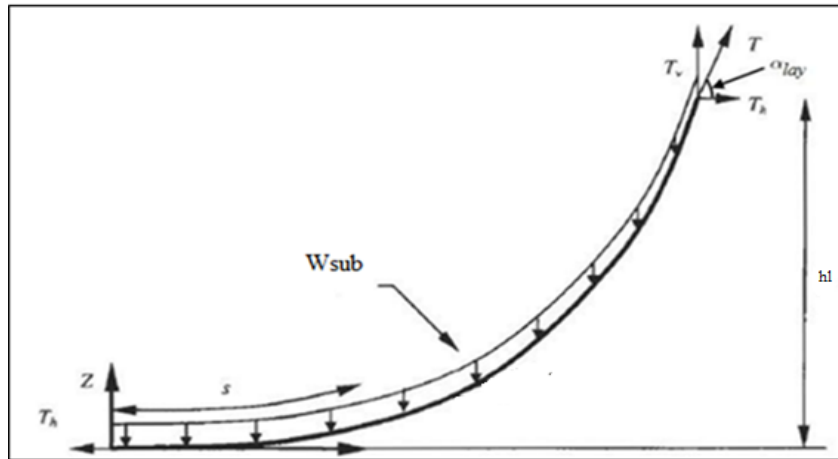
Figure. 5.17. Catenary Model of Pipeline [33]

Here, T- tension force, N; T_h, T_v – horizontal and vertical components of tension force, N; s – pipe length in free span, m; W_{sub} – weigh of submerged pipeline per unit length, N/m , h_l – water depth, m.

Figure 5.18 shows the stinger configuration, with the definition of the angles taken in the calculations.
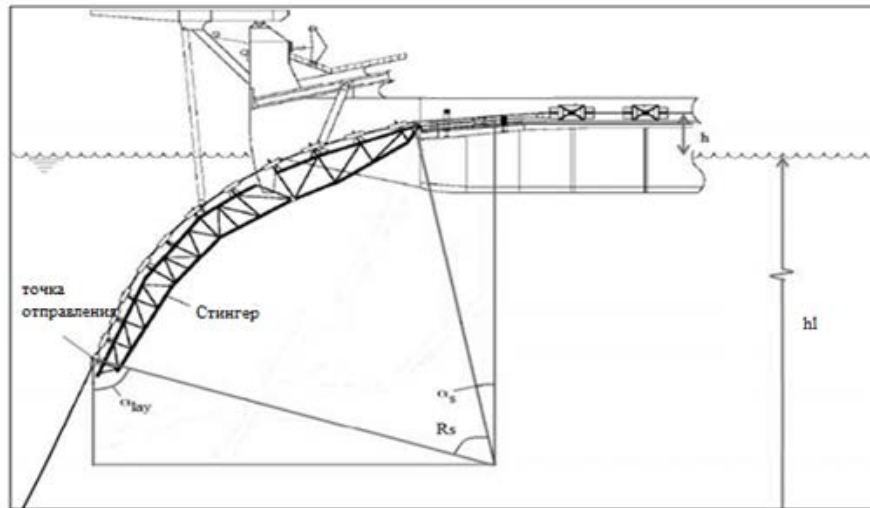
Figure 5.18. Stinger Geometry with Defined Angles [14]

The shape of the pipeline during its installation in the catenary model representation is described by the formula [33]:

$$z = a \cdot (\cosh \frac{x}{a} - 1) \tag{5.38}$$

In this equation, a can be interpreted as the radius of the curve in the sagbend at the touch down point [33]:

$$a = \frac{T_h}{W_{sub}} \qquad (5.39)$$

The distance from the departure point of the pipeline from the stinger to the touch down point is determined by the formula [33]:

$$x_{td} = a \cdot \cosh^{-1}\left(\frac{h_{mod} + a}{a}\right) \qquad (5.40)$$

where h_{mod} – where is the vertical distance between the seabed and the inflection point, m.

The vertical distance between the seabed and the inflection point is calculated as [33]:

$$h_{mod} = h_l + h - R_s \cdot (\cos\alpha_s - \cos\alpha_{lay}) \qquad (5.41)$$

where h – height above water, m; α_s – slight inclination, deg; α_{lay} – departure angle ,deg.

Pipe length in free span is determined as [33]:

$$s = h_{mod} \cdot \sqrt{1 + 2 \cdot \frac{a}{h_{mod}}} \qquad (5.42)$$

The horizontal component of the tension force is calculated by the formula [33]:

$$T_h = \frac{h_{mod} \cdot W_{sub}}{\tan(\alpha_{lay})^2} \cdot (1 + \sqrt{1 + \tan(\alpha_{lay})^2}) \qquad (5.43)$$

The vertical component of the tension force at the departure point is determined by the formula [33]:

$$T_v = w_s \cdot s \qquad (5.44)$$

The tension force parallel to the pipeline is defined as [33]:

$$T = \sqrt{T_v^2 + T_h^2} + W_{sub} \cdot R_s \cdot (\cos\alpha_s - \cos\alpha_{lay}) \qquad (5.45)$$

The maximum curvature in sagbend is calculated as [33]:

$$k_{sb} = \frac{1}{a} \qquad (5.46)$$

The maximum bending moment in sagbeng is calculated by the formula [33]:

$$M_{sb} = k_{sb} \cdot EI$$

where EI – pipe bending stiffness, N*m^2

The minimum horizontal lay radius can be expressed as [33]:

$$R_{lay} = \frac{T_h}{\mu \cdot W_{sub}} \qquad (5.47)$$

Maximum strain on stinger is calculated as [33]:

$$\varepsilon_s = \frac{D_o}{2 \cdot R_s + D_o} \qquad (5.48)$$

where R_s – stinger radius, m.

After all the parameters were determined, it is necessary to check displacement controlled - load combination of the pipeline on the stinger.

Pipe members subjected to longitudinal compressive strain (bending moment and axial force) and internal over pressure shall be designed to satisfy the following condition at all cross sections: [2]:

$$\varepsilon_d \le \frac{\varepsilon_c}{\gamma_\varepsilon} \qquad D/t \le 45, \; p_i < p_e \qquad (5.49)$$

where ε_d – design compressive strain, %; γ_ξ – strain resistance, ε_C – characteristic bending strain resistance, %.

Design compressive strain is calculated by the following formula [2]:

$$\varepsilon_d = \varepsilon_F \cdot \gamma_F \cdot \gamma_C + \varepsilon_E \cdot \gamma_E + \varepsilon_A \cdot \gamma_A \cdot \gamma_C \qquad (5.50)$$

where ε_F – compressive strain by functional loads, %; ε_A - compressive strain by accidental loads; ε_E – compressive strain by environmental loads; γ_F – functional load effect factor; γ_E – environmental load effect factor; γ_A – faccidental load effect factor; γ_C – condition load effect factor.

Load effect factors are determined by the Table 5.12; condition load effect factor is determined by the Table 5.13.

Table 5.12. Load effect factors and load combinations [2]

Limit State / Load combination			Functional loads	Environmental loads	Accidental loads
			γ_F	γ_E	γ_A
SLS и ULS		a	1.2	0.7	-
		b	1.1	1.3	-
FLS		c	1.0	1.0	-
ALS		d	1.0	1.0	1.0

Table 5.13. Condition load effect factors, γ_c [2]

Condition	γ_C
Pipeline resting on uneven seabed	1.07
Continuously stiff supported	0.82
Otherwise	1.00

Characteristic bending strain resistance ε_C is determined by the following formula [2]:

$$\varepsilon_c = 0.78 \cdot (\frac{t_2}{D} - 0.01) \cdot (1 + 5 \cdot \frac{\Delta p_d (D - t_2)}{2 \cdot t_2 \cdot f_y}) \cdot \alpha_h^{-1.5} \cdot \alpha_{gw} \qquad (5.51)$$

where Δp_d – difference between internal and external pressure, Pa; α_{gw} – girth weld factor, determined by the Figure 5.19; α_h – minimum strain hardening, for steel X70 can be taken equal to 0.92.
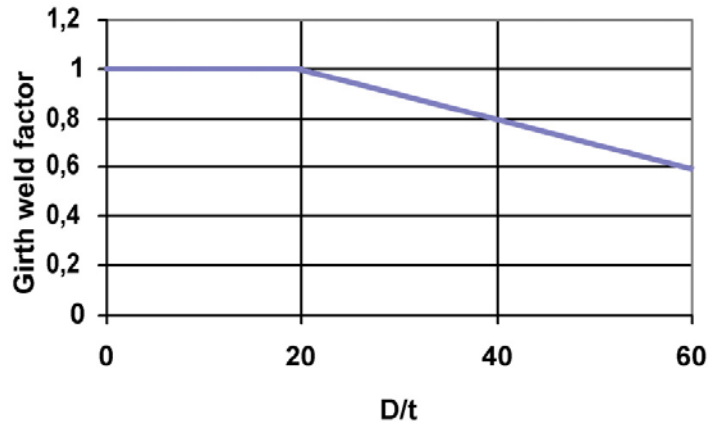
Figure 5.19. Proposed Graph for Girth Weld Factor [2]

The calculations were carried out with the following assumptions:

- Corrosion allowance $t_{corr} = 0$mm;
- No material derating due to elevated temperature;
- No internal nor external pressure;
- Functional compressive strain $\varepsilon_F = \varepsilon_s$;
- Environmental and accidental compressive strains ε_A, $\varepsilon_E = 0.0$;
- Load condition factor $\gamma_C = 1.00$;
- Safety Class = Normal.

From the formula (5.48), it can be seen that the stinger radius mainly affects the bending deformation of the pipe on the stinger.

After each element of the pipeline is checked for the criterion of displacement controlled - load combination of the pipeline on the stinger, it is necessary to check the pipeline sagbend section for the criterion of load controlled - load combination.

Pipe members subjected to bending moment, effective axial force and internal overpressure shall be designed to satisfy the following condition at all cross sections [2]:

$$\left(\gamma_{SC} \cdot \gamma_m \left(\frac{M_d}{\alpha_c \cdot M_p} \right) + \gamma_{SC} \cdot \gamma_m \left(\frac{S_d}{\alpha_c \cdot S_p} \right)^2 \right)^2 + \left(\gamma_{SC} \cdot \gamma \cdot \left(\frac{p_e}{p_c} \right) \right)^2 \leq 1 \quad D/t \leq 45, \ p_i < p_e \quad (5.52)$$

where M_d – design moment, N*m; S_d – the design effective axial force, N; M_p – plastic resistance moment, N*m; S_p – plastic resistance effective axial force, N; p_c – collapse pressure, Pa; α_c – flow stress parameter.

The design effective axial force is calculated by the formula [2]:

$$S_d = S_F \cdot \gamma_F \cdot \gamma_C + S_E \cdot \gamma_E + S_A \cdot \gamma_A \cdot \gamma_C \quad (5.53)$$

where S_F – effective axial force by functional loads, N; S_E – effective axial force by environmental loads, N; S_A – effective axial force by accidental loads, N.

The design moment is calculated as [2]:

$$M_d = M_F \cdot \gamma_F \cdot \gamma_C + M_E \cdot \gamma_E + M_A \cdot \gamma_A \cdot \gamma_C \quad (5.54)$$

where M_F – moment by functional loads, N*m; M_E – moment by environmental loads, N*m; M_A – moment by accidental loads, N*m.

The plastic resistance moment is determined by the formula [2]:

$$M_P = f_y \cdot (D - t_2)^2 \cdot t_2 \quad (5.55)$$

The plastic resistance effective axial force is calculated as [2]:

$$S_P = f_y \cdot (D - t_2) \cdot t_2 \quad (5.56)$$

The flow stress parameter α_c, is calculated as follows [2]:

$$\alpha_c = (1 - \beta) + \beta \cdot \frac{f_u}{f_y} \quad (5.57)$$

$$\beta = \begin{cases} 0.4 + q_h & \text{при } D/t_2 < 15 \\ (0.4 + q_h) \cdot (60 - D/t_2)/45 & \text{при } D/t_2 \leq 60 \\ 0 & \text{при } D/t_2 > 60 \end{cases} \qquad (5.58)$$

$$qh = \begin{cases} \dfrac{(p_{ld} - p_e) \cdot 2}{p_b(t_2) \cdot \sqrt{3}} & npu \ p_{ld} > p_e \\ 0 & npu \ p_{ld} < p_e \end{cases} \qquad (5.59)$$

The calculations were carried out with the following assumptions:

− Corrosion allowance $t_{corr} = 0$mm.

− No material derating due to elevated temperature.

− Internal pressure $p_i = 0$

− External pressure $p_e = \rho \cdot g \cdot h_l$

− Functional bending moment $M_F = M_{sb}$

− Environmental and Accidental bending moments M_E, $M_A = 0.0$

− Functional effective axial force $S_F = T_h$

− Environmental effective axial force $S_E = 0.0$

− Load effect factor $\gamma_C = 1.0$

− Safety Class = Normal.

The condition (5.52) is mainly influenced by the values of the maximum bending moment in sagbend M_{sb} and the horizontal component of tension force, which are depended on the values of the angles α_{lay} and α_s, as well as submerged weight of pipeline.

The calculation results for the pipeline section with a 50 mm concrete coating during installation at depth of 346 are presented below:

Table 5.14. Results of pipeline stress-strain analysis

Parameter	Value	Unit
Tension at vessel (T)	2.135	KN
Horizontal lay tension (T_h)	1.472	KN
Maximum strain on stinger (ε_s)	0.005	%
Maximum curvature in sagbend (k_{sb})	0.00126	1/m
Horizontal Distance from vessel to touch-down (x_{td})	695.45	m

Maximum moment in sagbend (M_{sb})	1842	KNm
Minimum horizontal lay radius (R_{lay})	1127	m
Utilization ratio on stinger	0.95<1	
Utilization ratio in sagbend	0.64<1	

In this section, the stress-strain state of the pipeline during its S-lay installation is made. Calculations were made for a section of a concreted pipeline with 50 mm thickness, during its installation at maximum depth (346 m). The pipeline sections were checked for the criterion of combined loading on the stinger and in the sagbend. The obtained values of utilization rations (<1) indicate that installation of pipeline is possible without any additional technological solutions.

5.7. Flow Assurance Aspects

When designing the offshore pipeline for the Shtokman gas condensate field, one of the main issue is to ensure a continuous flow of hydrocarbons from the floating production unit to the onshore facilities. For the Shtokman project, three options for transporting of raw materials were considered:

– Single-phase flow (gas by pipeline; condensate by tankers);
– Three-phase flow (gas + water + condensate);
– Dry two-phase flow (dehydrated gas + condensate).

In April 2011, the Board of Directors of «Shtokman Development AG» approved the two-phase flow, with onshore separation of gas and condensate [42]. This option of transporting raw materials to the shore significantly reduces the cost of project implementation compared with single-phase flow regime. In single-flow regime, a mixture of gas and condensate is lifted vertically into the process tankers, where the condensate is separated from the gas and transported by special vessels, while the gas is pumped by pipelines to the shore. In this case, it is necessary to provide a separate delivery methods for each of the products, this leads to an increase in the cost of the project.

The advantages of a two-phase flow compared to a three-phase flow include:

– Liquid transportation in two-phase flow is more efficient;
– Modelling of two-phase flow is less complex and more confident than modelling of three-phase flow;

81

There are main flow assurance risks for Shtokman trunk pipeline such as formation of gas hydrates and water accumulation.

Hydrate management

Hydrate formation in the Shtokman pipeline is possible due to following factors [34]:

  – High reservoir pressure (approximately 200 bar);
  – Low minimum ambient temperature: (-1.8 °C at seabed / -31°C onshore);
  – Gas is saturated with water at reservoir conditions.

To prevent hydrate formation, it is necessary to perform primary gas treatment including gas dehydration at the Floating Production Unit. A dehydration specification of 6 ppm mol water in the fluid at the outlet of dehydration is specified [34]. The planned Scheme of Shtokman Offshore Gas Treatment is presented in the Figure 5.20.
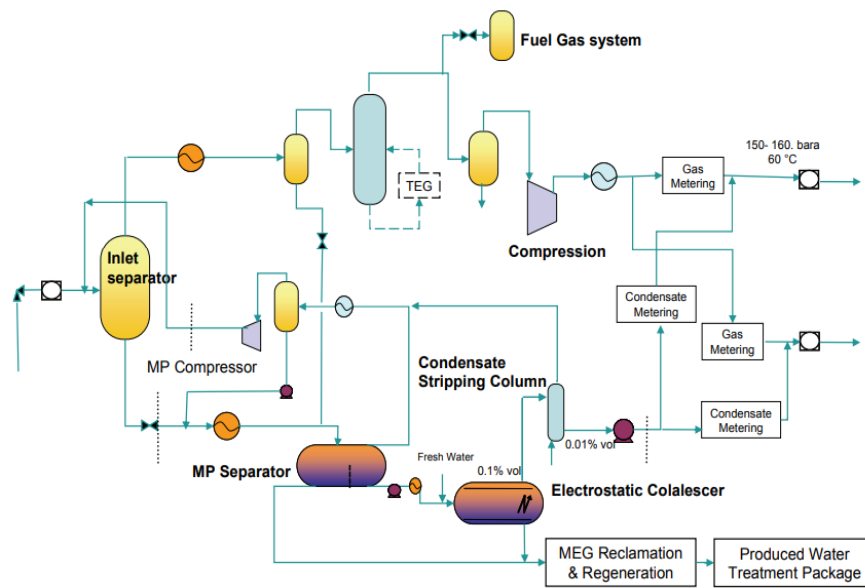

Figure 5.20 Scheme of Shtokman Offshore Gas Treatment [10]

It is also necessary to use hydrate formation inhibitors. Usually glycols are used as hydrate formation inhibitors. According to [34], the approximate required monoethylene glycol (MEG) concentration in produced water is equal to 60 wt%. However, the amount of required MEG may vary depending on reservoir temperature, water saturation and MEG quality. The phase diagrams of hydrate formation for pay zones J_0 and J_1 of SGCF (initial conditions/ with inhibitors) are presented in the Figure 5.20.
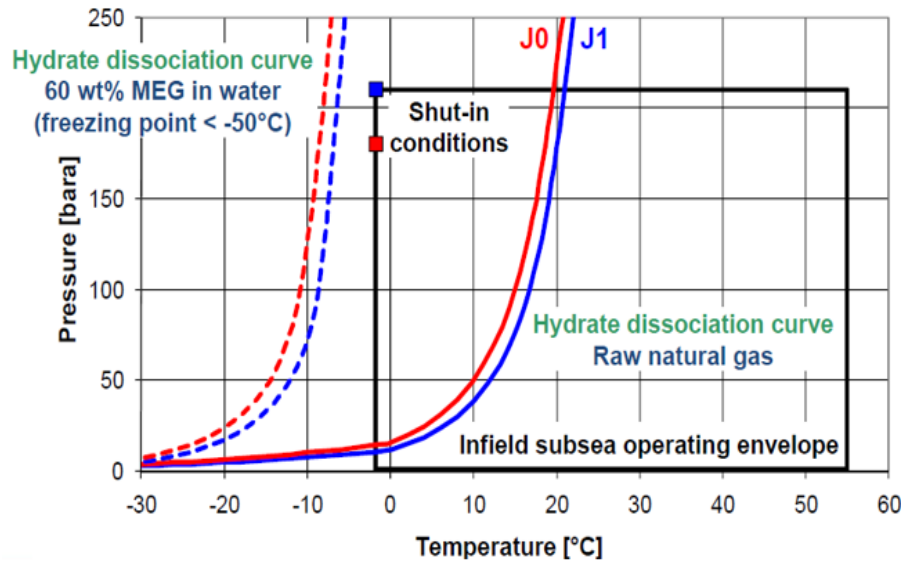
Figure 5.21 Phase Diagram of Hydrate Formation for SGCF [34]

Liquid management

In dry two-phase gas-condensate pipelines, the gas throughput must be maintained at a level that exceeds the minimum flow rate (turndown rate) to avoid the accumulation of large volumes of liquid. A pipeline can be operated below the turndown rate, if the total accumulation of fluid remains below a permissible limit. To prevent the shutdown of production initiated by the fast production of large liquid volumes, a slug catcher is installed at the outlet of gas-condensate pipelines. For Shtokman case, a trap for finger-type mucus was selected with a total capacity of 2500 m³ in order to adapt to a wide range of working conditions, fluid loads and transients (buildup, restart, cleaning) [34].

The slug catcher is one of the key elements of a liquid management strategy. Another key element is the work philosophy. Since two 36-inch highways share the same facilities at their ends, a special working philosophy was developed to minimize fluid retention in the lines. Essentially, the produced condensate is preferably distributed along a trunk line with a maximum capacity. After the first gas operation, the procedures will be corrected with the support of multi-phase dynamic simulation [34].

6. Safety and Environment

When designing any structure, it is extremely important to work out possible scenarios in advance and assess the risks during the construction phase as well as during operation. Of course, the offshore pipeline is not an exception, but rather refers to potentially dangerous objects for the environment and working personnel, especially when we talk about Arctic regions with very sensitive ecology system.

This chapter describes the main necessary measures to protect the environment during construction and operation of offshore pipelines in accordance with Russian set of rules SP 378.1325800.2017 «The offshore pipelines. Design and construction» [28].

All types of work related to the construction and operation of the offshore pipeline should be based on a careful selection of technological processes, technical means and equipment ensuring the safety of the ecological environment of the construction region. Only those technological processes should be used that will ensure the permissible environmental impact and its restoration after the completion of the offshore pipeline construction [28].

Project documentation must contain a section «Environmental Protection» with an environmental impact assessment. Evaluation should be carried out for natural components (geological environment, water, air, soil, vegetation, wildlife) and natural complexes (landscapes) in a strip equal in width to the zone of the pipeline's influence on natural components and complexes [28].

The assessment should be carried out in volumes sufficient to determine the environmental risk associated with the possibility of causing damage to the life and health of the population (risk in case of accidents), rare and endangered species of animals and plants (risk of loss of the gene pool); natural resources. The main design decisions on the protection of the environment and the protection of the population should be coordinated with the representatives of the public of the settlement located in the immediate vicinity of the offshore pipeline route [28].

When designing, it is necessary to foresee the construction of environmental facilities, the creation of a network of temporary roads, driveways and parking places for construction equipment, as well as measures to prevent environmental pollution from construction, household waste, fuel and lubricants [28].

In the construction of offshore pipelines in areas of commercial fishing importance, measures should be taken to preserve and restore biological resources [28].

The start and end dates of underwater ground works using jetting or blasting must be performed with accordance of the fish protection authorities recommendations, based on the timing of spawning, feeding, fish migration, and the development cycles of plankton and benthos in the coastal zone [28].

A safety system should be provided for the offshore pipeline that will prevent or minimize the effects of overpressure, leakage and damage of pipeline.

During the operation of the offshore pipeline, it is necessary to predict the possibility of pipeline burst and product release with an estimate of the expected damage to sea biota and implement the protective measures provided for such cases in the project documentation [28].

To protect and preserve the natural environment in the sea and in the coastal zone, it is necessary to organize constant supervision over the observance of environmental protection measures during the entire period of anthropogenic impact caused by the performance of work during the construction and operation of the subsea pipeline [28].

Conclusion

At present, Russia faces the task of industrial development of oil and gas reserves on the Arctic shelf. Russia, which in turn requires the creation of the largest offshore pipeline system.

In general, the construction of offshore pipelines in the Arctic region requires the solution of a number of tasks, including technical, technological and organizational, which are associated with significant difficulties caused by natural conditions, remoteness from industrialized areas, lack of developed infrastructure and strict environmental requirements.

In this master's thesis, an analysis of the prospects for developing the Arctic shelf of Russia was carried out, as a result of which it can be concluded that the Barents-Kara region is the most promising area for development, in terms of technical and economic indicators.

An analysis of the world practice of the construction of subsea pipelines in the Arctic and subarctic regions was conducted.

The main features and problems during the construction and operation of underwater pipelines in the Arctic are described, and methods for their solution are proposed.

Master's thesis includes such stages of subsea pipeline design as calculation of minimum wall thickness of pipeline as well determination of required weighting concrete coating thickness along the entire length of pipeline. The calculations were carried out evidence from the trunk pipeline for the Shtokman gas condensate field (SCGF – Teriberka).

As a result of the calculations, it was established that the minimum wall thickness of the pipeline is 25.1 mm.

To ensure the on-bottom stability of the pipeline, the first 407 km must be covered with 50mm concrete coating, in the coastal area the pipeline must be covered with a 150 mm concrete coating, additionally, it must be trenched, to avoid high hydrodynamic loads of waves and currents in shallow water.

The analysis of stress-strain state of concrete coated pipeline during its installation at maximum depth of 346m showed the possibility of installation by S-lay method, without any additional technological solutions.

References

1. Barrette, P., Barker, A., Gardin, E. (2018). The Subsea Drake Pipeline: A Challenging Case Study to Check Design Effectiveness Against Drifting Ice Action. Offshore Technology Conference. doi:10.4043/29175-MS.

2. DNV-OS-F101 (2007). Offshore standard. «Submarine pipeline systems», Det Norske Veritas.

3. DNV-RP-E305 (1988). Recommended practice «On-bottom stability design of submarine pipelines», Det Norske Veritas.

4. Eisler, B. (2011). Leak Detection Systems and Challenges for Arctic Subsea Pipelines. Offshore Technology Conference. doi:10.4043/22134-MS.

5. Eisler, B. (2016). Shore Crossing Design Considerations & Solutions for Arctic Subsea Pipelines. Offshore Technology Conference. doi:10.4043/27453-MS

6. Girdyuk, G.V., Dzhenyuk, S.L., Zykova, G.G., Terziev, F.S (1990). Hydrometeorology and hydrochemistry of the USSR seas, the Barents Sea, vol. 1, Hydrometereological Conditions. Publishing house: Gidrometeoizdat, Leningrad, 280 p.

7. Lanan, G. A., Cowin, T. G., Johnston, D. K. (2011). Alaskan Beaufort Sea Pipeline Design, Installation and Operation. Offshore Technology Conference. doi:10.4043/22110-MS.

8. Ivanets, D. V. (2000). Development of Methods of Selection of Perspective Technologies of Construction of Sea Pipelines on the Arctic Shelf. PhD thesis, Gubkin Russian State University of Oil and Gas, Moscow.

9. Hamilton, J., Prescott, N. (2014). Arctic Subsea Pipelines and Subsea Production Facilities. Topic Paper, Prepared for the National Petroleum Council Study on Research to Facilitate Prudent Arctic Development.

10. Holm, H., Saha, P., Suleymanov, V., Vanvik, T., & Hoyer, N. (2011). Shtokman Flow Assurance Challenges – A Systematic Approach to Analyze Uncertainties – Part 1. BHR Group.

11. Jukes, P., Kenny, S., Panapitiya, U., Jafri, S., Eltaher, A. (2011). Arctic and Harsh Environment Pipeline Trenching Technologies and Challenges. Offshore Technology Conference. doi:10.4043/22083-MS.

12. Karunakaran, D. (2019). Pipelines and risers lecture notes. University of Stavanger.

13. Kazanin, G.S., Ivanov G.I., Zayats I.V. (2015). Innovative Geological-geophysical Studies of Marine Arctic Geological Expedition at the shelf of Arctic. International scientific-practical conference «New ideas in oil and gas geology – 2015», pp 134-140.

14. Kyriakides, S., Corona, E. (2007). Mechanics of offshore pipelines: Volume 1. Amsterdam: Elsevier.

15. Lange, F., Van Zandwijk, K., & van der Graaf, J. (2011). Offshore Pipeline Installation In Arctic Environment. Society of Petroleum Engineers. doi:10.2118/149581-MS

16. Lopatukhin, L.I. (2013). Reference data on the wind and waves of the Barents, Okhotsk and Caspian seas. Russian Maritime Register of Shipping, Saint Petersburg, 335p.

17. Løset, S., Shkhinek, K., Gudmestad, O. T., Strass, P., Michalenko, E., Frederking, R., & Kärnä, T (1999). Comparison of the physical environment of some Arctic seas. Cold Regions Science and Technology, 29(3), pp 201-214.

18. Paulin, M., Cocker, J., Humby, D., Lanan, G. (2014). Trenching of Pipelines for Protection in Ice Environments. Offshore Technology Conference. doi:10.4043/24606-MS.

19. Paulin, M. (2014). Arctic Offshore Pipeline Design and Installation Challenges. Offshore Technology Conference. doi:10.4043/24607-MS.

20. Nikitin, B.A., Dzyublo, A.D. (2017). Prospects for the Development of Gas Resources on the Shelf of the Arctic Seas of Russia. Vesti Gazovoy Nauki, 4 (32), pp 15-24.

21. Papusha, A., Kazunin, D., Gontarev, D., Vasilevich, V., Kyalbieva, S. (2013). Stability and Strength of the Subsea Pipeline Under Iceberg Load in Arctic. Society of Petroleum Engineers. doi:10.2118/166941-MS.

22. Rosneft, the Editors: Pavlov V., et al. (2015). Atlas of hydrometeorological and ice conditions in the Russian Arctic seas: the generalization of library materials and the results of the field research of "Arctic Research and Design Center for Offshore Development" in 2012-2014.Oil Industry. Moscow.

23. Sarpkaya, T. and Isaacson M. (1981). Mechanics of Wave Forces on Offshore Structures, Van Nostrand Reinhold. New York.

24. «Shtokman Development AG», «Frecom» Ltd (2010). Complex Development of the Shtokman Gas-Condensate Deposit. Phase 1. Report.

25. SJK «Sevmorneftegas». (2007). Adjustments to the Shtokman gas and condensate field development project.

26. Sklyar, M.I. (2007). Shtokman gas condensate field: problems and development prospects. National Interests: Priorities and Security, (12), pp 47-54.

27. Skorobogatov, V.A. (2015). Gas Potential of Arctic seas in Northern Eurasia: Amount, Structure, Prospects for Exploration and Development in the XXI Century. All-Russia conference «Arctic – Oil and Gas 2015», pp 23-28.

28. SP 378.1325800.2017 (2017). Set of rules. «The offshore pipelines. Design and construction».

29. Suprunenko, O.I. (2006). Marking out New Objects of High Oil and Gas Potential Using Complex Geologic-geophysical Models of the Laptev-Sea Sedimentary Basins. Geology of oil and gas, 13(2), pp 35-41.

30. Thusyanthan, I., Wang, J & Haigh, S. (2017). Cyclic Ratcheting Resistance of Buried Pipelines. 10.4043/27823-MS.

31. Tomareva, I. A. (2014). Design and technological features of underwater pipelines construction. Publishing house: Volgograd, Volgograd, 91 p.

32. Vasiliev, G.G., Goryainov, Y. A., Bespalov, A.P. (2015). The construction of offshore pipelines. Publishing house: Gubkin Russian State University of Oil and Gas, Moscow, 200 p.

33. Wedin, H. (2012). Limit State Criterion Theory for Pipeline Subsea Installation Processes. Master's Thesis. KTH, School of Engineering Sciences (SCI).

34. Zakarian, E., Holm, H., Saha, P., Lisitskaya, V., Suleymanov V., (2009). Shtokman: the Management of Flow Assurance Constraints in Remote Arctic Environment.

35. Zubakin, G.K. et al. (1994) Ice Conditions and Icebergs in the area of the Shtokman gas Condensate field on the Gas Pipeline Routes. Feasibility Study for the Development of SGCF, vol. 5. Saint-Petersburg, 345 p.

36. Zubakin, G.K., Naumov, A.K., Buzin, I. (2004). Estimates of ice and iceberg spreading in the Barents Sea. Proceedings of the International Offshore and Polar Engineering Conference, pp 863-870.

37. Link: http://offshoremarintec-russia.ru/

38. Link: http://trans.lukoil.ru/ru/

39. Link: http://www.gazprom.ru

40. Link: http://www.shtokman.ru/

41. Link: https://bnews.kz

42. Link: https://teknoblog.ru

43. Link: https://www.subsea7.com

44. Link: https://www.worldatlas.com

45. Link: https://www.sputniknews.com